INSTITUT d'OPTIQUE GRADUATE SCHOOL ParisTech | LEnsE Laboratoire d'Enseignement Expérimental

Lab work in photonics

Quantum photonics

Rooms	**P1**	**P2**	**P3**	**P4**	**P5**
	N1.3	S1.29	N1.3	N1.4	N1.6

lense.institutoptique.fr / Troisième année/ Photonique 3A|M2

Engineer - 3rd year - Palaiseau

Master 2 QLMN
Year 2024-2025

P 1

Entangled photons and Bell's inequality

Questions P1 to P11 have to be done before the class.

Contents

1 Introduction

Quantum theory does not allow one to calculate the outcome of a measurement, but rather the probability of the different possible outcomes. Because of this probabilistic aspect, many physicist, including Einstein, were dubious and thought that quantum mechanics had to be an incomplete theory that was not accounting for the full reality. To illustrate this point, Einstein, Podolski and Rosen presented in 1935 a "gedankenexperiment" (mental experiment) where a measurement on an entangled two-particle state (Bell state or EPR state) lead to a paradox, which the authors interpret as a proof of the incompleteness of the quantum theory [1].

For a Bell state, a measurement of the state of each particle taken individually gives a random outcome, but the results on the two particles are perfectly correlated. In other words, a measurement of the first particle state allows us to predict with certainty the state of the second one. For Einstein, Podolsky and Rosen, the possibility of predicting the state of the second particle implies that this state exists before the measurement, implying that there is a set of "hidden" variables (in the sense that they are not described by the theory) that determine this state all along the experiment.

For a long time, it has seemed that the debate between an hidden variable interpretation and a purely probabilistic theory was a philosophical discussion. However, in 1964, John Bell [2] showed that there were some cases where the two interpretations were leading to incompatible observations, and that it was possible to settle the debate with an experiment. But it has

[1] A. Einstein, B. Podolsky et N. Rosen, *Can Quantum-Mechanical Description of Physical Reality Be Considered Complete?*, Physical Review **47**, 777 (1935)

[2] J. S. Bell, *On the Einstein-Podolsky-Rosen paradox*, Physics **1**, 195 (1964)

been necessary to wait 15 more years for the progress in **quantum optics** to implement this experiment with pairs of entangled photons. The first unambiguous results have been obtained at the Institut d'Optique by Alain Aspect, Philippe Grangier and Jean Dalibard [3].

This lab work, inspired by **M. W. Mitchell** and **D. Dehlinger**, aims to produce a two-photons Bell state, and allows you to determine, with your own measurements, which theory can be invalidated.

2 Bell states

2.1 Polarization state of a photon in quantum mechanic

When we measure the polarization of a photon with a vertical analyzer, we refer to the basis formed by the vertical polarization ($|V\rangle$ parallel to the analyzer axis) and the horizontal polarization ($|H\rangle$ orthogonal to the analyzer axis). In this basis, the polarization state is written:

$$|\psi\rangle = c_V|V\rangle + c_H|H\rangle\,. \tag{1.1}$$

The coefficients c_V and c_H are complex number such as $|c_V|^2 + |c_H|^2 = 1$. The measurement of the photon polarization can only gives two outcomes:

- The photon is transmitted by the polariser and its polarization state is projected on $|V\rangle$. Quantum mechanics predicts that the probability of this result is $P_V = |\langle\psi|V\rangle|^2 = |c_V|^2$;
- The photon is blocked by the polariser and its polarization state is projected on $|H\rangle$. The associated probability is $P_H = |\langle\psi|H\rangle|^2 = |c_H|^2$.

P1 Write the polarization state of a photon with a rectilinear polarization, at an angle α from the vertical. What is the probability to measure it in the state $|V\rangle$?

P2 Write the polarization state of a photon with a left-circular polarization. What is the probability to measure it in the state $|V\rangle$?

If we choose to measure the polarization state of a photon with a polariser rotated by an angle α from the vertical, the new basis of the polarization state is $\{|V_\alpha\rangle, |H_\alpha\rangle\}$ (figure 1.1).

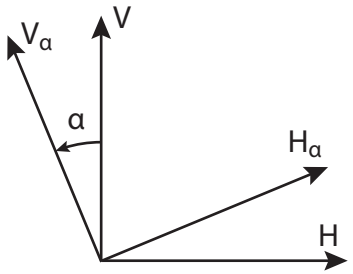

Figure 1.1 – The basis of the polarization state $\{|V_\alpha\rangle, |H_\alpha\rangle\}$ is obtained by rotating the basis $\{|V\rangle, |H\rangle\}$ by an angle α.

[3] See for instance : A. Aspect, J. Dalibard et G. Roger, *Experimental Test of Bell's Inequalities Using Time-Varying Analyzers*, Physical Review Letters **49**, 1804 (1982)

P3 Consider a photon in the polarization state $|V\rangle$. Write its state in the basis $\{|V_\alpha\rangle, |H_\alpha\rangle\}$. What is the probability P_{V_α} of measuring the polarization V_α?

2.2 Pairs of polarization-entangled photons

During this lab work, you will produce and characterize pairs of polarization-entangled photons. The polarization state of those pairs is a Bell state, written as follow:

$$|\psi\rangle = \frac{1}{\sqrt{2}} \left(|V, V\rangle + |H, H\rangle\right) . \tag{1.2}$$

It is a non separable state, which means that we can not assign a polarization state to each photon individually.

P4 Show that the probability P_V of measuring the photon 1 **or** the photon 2 in the polarization V is 1/2.

P5 What is the probability of measuring the two photons in the same polarization state (V, V or H, H)? What is the probability of measuring the two photons in orthogonal polarization states (V, H or H, V)?

In other words, a polarization measurement on one of the photons gives a random result, but if we measure the polarizations of the two photons of the pair, the results are always **correlated**. More generally, the probability to measure simultaneously the photon 1 in the polarization state V_α and the photon 2 in the polarization state V_β is given by

$$P(V_\alpha, V_\beta) = |\langle V_\alpha, V_\beta|\psi\rangle|^2 . \tag{1.3}$$

P6 Show that $P(V_\alpha, V_\beta) = \cos^2(\alpha - \beta)/2$. How does this probability change when the two axis of analysis are rotated by the same angle?

P7 Show that the Bell state has the same form than (1.2) no matter what the basis of analysis is, which implies that:

$$|\psi\rangle = \frac{1}{\sqrt{2}} \left(|V_\alpha, V_\alpha\rangle + |H_\alpha, H_\alpha\rangle\right) , \quad \forall\alpha . \tag{1.4}$$

This **rotational symmetry** of the polarization state is a crucial property of the Bell state that we will use to reveal the full extent of the correlation between the entangled photons.

2.3 Bell's inequality

For arbitrary orientated analyzers, the degree of correlation between the results of the measurements on the two photons can be quantified by the quantity

$$E(\alpha, \beta) = P(V_\alpha, V_\beta) + P(H_\alpha, H_\beta) - P(V_\alpha, H_\beta) - P(H_\alpha, V_\beta) . \tag{1.5}$$

From this quantity, we can define the **Bell parameter** :

$$S(\alpha, \alpha', \beta, \beta') = E(\alpha, \beta) - E(\alpha, \beta') + E(\alpha', \beta) + E(\alpha', \beta')\,. \tag{1.6}$$

It is that parameter that allows one to distinguish between the hidden variable theory and the quantum theory. Indeed, Bell showed that according to the hidden variable theory, S should be lower than 2 no matter the state of the two photons. It is the so-called **Bell inequality**. On the other hand, the quantum theory predicts a value of S strictly greater than 2 for a Bell state, for a certain choice of angles of analysis.

P8 Show that $S = 2\sqrt{2}$ for the set of angles of analysis depicted in figure 1.2. In this configuration, the Bell inequality are maximally violated by quantum mechanics.

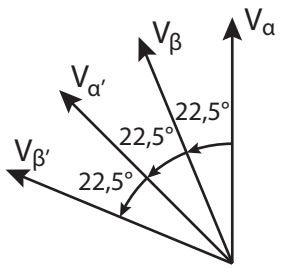

Figure 1.2 – This set of angles of analysis maximizes the Bell parameter predicted by quantum mechanic.

3 Experimental implementation

3.1 Description of the experiment

The source of polarization-entangled photons consists in a laser diode emitting a $405\,\mathrm{nm}$ beam, vertically polarized and focused on two non-linear crystals of BBO. In those crystals, a parametric conversion process turn the $405\,\mathrm{nm}$ photons into a pair of $810\,\mathrm{nm}$ photons. One of the crystal generates pairs of photons with a vertical polarization, and the other one generates a horizontally-polarized pair. The twin photons are emitted symmetrically with respect to the probe beam, inside a cone with an aperture of about $3°$. An half-wave plate working at $405\,\mathrm{nm}$ and a Babinet compensator allows one to adjust the polarization state of the probe beam.

To collect the infrared photons, we use an avalanche photodiode (APD) on both side of the emission cone. Before entering into the detector, the infrared photons go through a polarization analyzer made of an half-wave plate, a polarization beam splitter (PBS), a lens to focus the beam onto the photodiode, and a interferential filter centered on $810\,\mathrm{nm}$ with a $10\,\mathrm{nm}$ width. A FPGA card is used to count the number of photons detected, as well as the number of coincidences, which correspond to a simultaneous detection on both arms. Those measurement are then displayed by a Labview code.

3.2 Single photons detection device

The detection devices are made of silicon APD used in single photon detection mode. On each arm A and B, the detection of a photon produce a TTL pulse ($0\,\mathrm{V}$ to $5\,\mathrm{V}$) with a temporal width of $25\,\mathrm{ns}$.

Warning ! Those detectors are very, very expensive and would be destroyed by a strong photon flux! Always check that the black tubes and the filters are installed to protect the photodiodes. Wait for the teacher authorization to switch on the detectors, and make sure that the main lights are off and the door is closed.

3.3 Events and coincidences counters

The FPGA card counts the TTL pulses emitted by the detectors (after a conversion from $0\,\mathrm{V}$ to $5\,\mathrm{V}$ to $0\,\mathrm{V}$ to $3{,}3\,\mathrm{V}$), and the number of coincidences between the A and B pulses within an adjustable integration time. To count the coincidences, the FPGA card proceeds as follows: when a pulse arrives on channel A, a time window of adjustable duration is open; if a pulse arrives on channel B before this window is closed, a coincidence is counted. The card send the counting information to the computer via a RS232 link, and the information is displayed by a Labview code. All the connections are already done, and we payed attention to the fact that the cables linking the APD to the coincidence counters have the same length.

Q1 Why do the cables need to have the same length?

$\rightsquigarrow$ Make the following settings:

- Before doing anything else, switch on the FPGA card, then start the Labview program and:
- Switch off every lights and turn the photons counters on.
- Measure the number of dark counts. The lower this number is, the better the detectors are.
- Switch a weak light and check that the number of detected photons stays well below $10^6\,\mathrm{photons/s}$.

3.4 Number of accidental coincidences.

For now, since the light sources are chaotic, the photons arriving in A and B are not correlated, and therefore the potential coincidences that you might detect are accidental. We note n_A and n_B the **counting rate** (average number of photons per second) on channels A and B, n_f the rate of accidental coincidences, and τ, the duration of the coincidence window.

Q2 Show that the rate of accidental coincidence is given by : $n_\mathrm{f} = n_A\, n_B\, \tau$.

The last two switches of the FPGA card, SW16 and SW17, allows one to choose the duration of the coincidence window (see table 3.1). The number given by this table are approximative and need to be re-measured.

SW16	SW17	τ (ns)
off	off	~ 70
on	off	~ 20
off	on	~ 14
on	on	~ 7

Table 1.1 – Duration of the coincidence window.

$\rightsquigarrow$ Measure the rate of accidental coincidences for each of the four configurations.

Q3 Calculate the durations of the four coincidence windows using the formula established in question **Q2**.

This measure allows one to check the behavior of the coincidence counters. Call the teacher if the results are way different from the value of table 3.1.

3.5 Pump diode

The pump diode is a $405\,\mathrm{nm}$ laser with about $60\,\mathrm{mW}$ of output power. The light emitted by the diode is linearly polarized. The wearing of security glasses is mandatory!

$\rightsquigarrow$ Make the following settings:

- Press the two buttons to turn on the temperature regulator of the diode. The temperature is already set to obtain the correct wavelength. Don't try to change it.
- Press the two buttons to turn on the current supply of the diode, and set the current at maximum (about $95\,\mathrm{mA}$).
- If they are present on the bench, remove the optical elements mounted before the BBO crystals (half-wave plates at $405\,\mathrm{nm}$ and Babinet compensator) as well as the half-wave plates at $810\,\mathrm{nm}$ and the PBS cubes in front of the detection channels.
- Check the alignement of the beams (they should be already well aligned).

3.6 Parametric conversion

The photon pairs are produced by parametric down conversion in non-linear crystals β-$\mathrm{BaB_2O_4}$ (baryum β-borate, BBO for short). During the non-linear process, a photon of the $405\,\mathrm{nm}$ pump can be converted in a pair of twin $810\,\mathrm{nm}$ photons. The BBO is a negative uniaxial

birefringent crystal. We use a type I phase matching, meaning that the twin photons have the same polarization.

The pump beam is orthogonal to the entrance plane of the crystals. The optical axis of the crystals makes an angle of about 29° with the pump beam. The optical axis of the first crystal and the axis of the pump are forming a vertical plane, and the $810\,\mathrm{nm}$ twin photons emitted from this crystal are horizontally polarized (see figure 3.3). The optical axis of the second crystal and the axis of the pump are forming a horizontal plane, and the twin photons are emitted with a vertical polarization. In both cases, the twin photons are emitted symmetrically with respect to the pump axis, within a cone of about 3° of aperture.

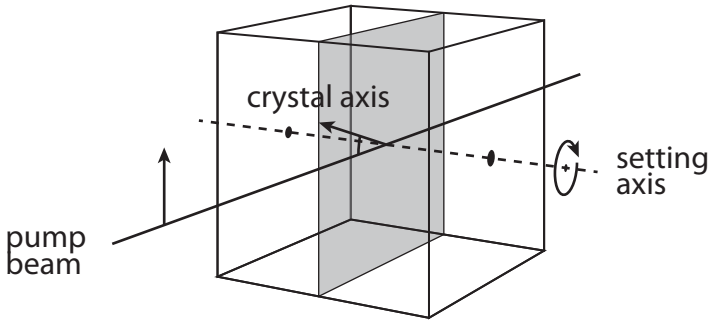

Figure 1.3 – The optical axis of the crystal is oriented "vertically" with respect to the pump axis. The other crystal is oriented "horizontally".

Note: The direction of emission of the twin photons varies very quickly with the angle between the crystal axis and the pump axis. To optimize the number of twin photons arriving onto the detectors, one should carefully set the orientation of the two crystals, using the horizontal and vertical screws of the mount (see figure 3.3).

3.7 Settings of the collimation lens

To efficiently detect the pairs, the waist of the pump beam (which is inside the BBO crystals) is imaged onto the APD's sensitive surface. It is a difficult setting because this surface has a diameter of $180\,\mu\mathrm{m}$ only. The lenses have a focal length of $75\,\mathrm{mm}$ and a diameter of $12{,}7\,\mathrm{mm}$. They are mounted $1040\,\mathrm{mm}$ away from the crystal.

Q4 Calculate the position of the image of the waist.

$\rightsquigarrow$ Check that the APD are approximatively at this position.

Q5 What is the magnification? Give an estimation of the diameter of the waist, then check that the size of the sensitive area of the photodiode is not limitating.

3.8 Optimization of the coincidence number

The direction of emission of the twin photons is very sensitive to the orientation of the crystals, which needs to be carefully optimized. The pump beam being vertically polarized, only the

crystal whose axis is in a vertical plane can satisfy the phase matching condition for now. Its orientation can be adjusted thanks to the horizontal screw.

$\rightsquigarrow$ Optimize the number of coincidences by tuning the screw.

Q6 Calculate the number of accidental coincidences. Do we need to take it into account?

Q7 Calculate the ratio between the number of coincidences and the number of photons detected on each channel. Comment.

$\rightsquigarrow$ We will now optimize the orientation of the crystal whose axis is in an horizontal plane :

- Put the $405\,\mathrm{nm}$ half-wave plate before the BBO crystals.
- **Carefully identify the own axis of the plate (they do not correspond exactly to the 0 and $90°$ position). A good identification is crucial for the following**.
- Check that the number of coincidences is unchanged if the axis of the plate are horizontal and vertical. Explain why.
- Turn the plate at $45°$ to align the polarization of the pump beam with the horizontal axis.
- Optimize the number of coincidences by touching the vertical screw of the crystals.

3.9 $810\,\mathrm{nm}$ polarization analyzer

$\rightsquigarrow$ Put the $810\,\mathrm{nm}$ half-wave plates and the PBS cubes on each channel. Together they form a polarization analyzer (see figure 1.4).

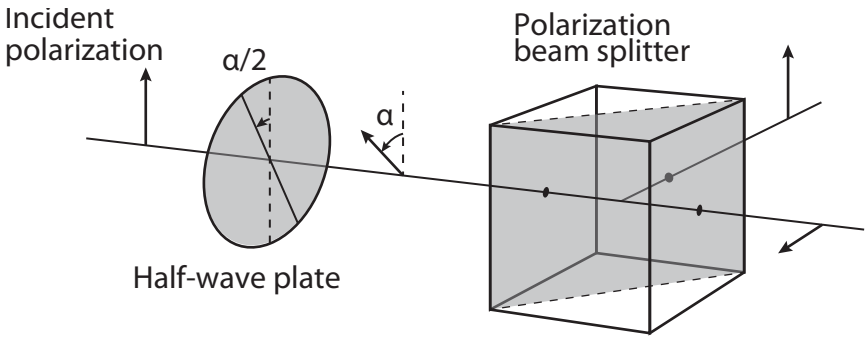

Figure 1.4 – The polarization analyzer is made of an half-wave plate (whose orientation is adjustable) and a PBS cube.

Warning : The angle of the analyser is equal to the angle of analysis divided by two. So be careful to distinguish the angle of analysis from the angle of the plate!

Q8 Show that when the plate is vertical, the analyzer transmits the horizontal polarization, and therefore allows to detect the $|H\rangle$ photons. How much do you need to turn the plate to detect $|V\rangle$ photons?

$\rightsquigarrow$ Settings and adjustments:

- Check experimentally that the twin photons are in the state $|H\rangle_1 |H\rangle_2$ if the $405\,\mathrm{nm}$ half wave plate is vertical, and in the state $|V\rangle_1 |V\rangle_2$ if the plate is rotated by $45°$.
- If necessary, turn again the screws of the BBO crystals to have approximatively the same number of coincidences for those two positions of the plate.
- Then set the plate to $22{,}5°$ (try to be very precise) to obtain approximatively the same number of coincidences with the two analyzers in vertical position and the two analyzers in horizontal position (it is impossible to obtain a perfect equality, but try to balance the coincidences as much as you can).

$\rightsquigarrow$ Measure the number of coincidences when the two analyzers are parallel (horizontally or vertically). Measure the number of coincidences when the two analyzers are orthogonal.

$\rightsquigarrow$ Adjust the angle of the half-wave plate to obtain the same rate of coincidence in both situations.

$\rightsquigarrow$ Measure the coincidence rates when the two analyzers are parallel and perpendicular in the diagonal base (at $45°$).

$\rightsquigarrow$ Note the absolutely astonishing result of this measurement!

Q9 What results were you expecting? Compare with the previous measurement.

The previous settings produced a source of photon pairs created in either crystal equiprobably. This is a pair of entangled photons! Now you need to precisely adjust the polarisation state of the pump beam to obtain a Bell state.

3.10 Realization of a Bell state

For now, your twin photons are in the state

$$|\psi\rangle = \frac{1}{\sqrt{2}} \left(|V, V\rangle + e^{i\phi} |H, H\rangle \right) . \tag{1.7}$$

Where ϕ is the phase difference between the twin photons horizontally polarized, and the twin photons vertically polarized. This phase difference is linked to the birefringence of the BBO crystals.

Q10 Calculate the join probability $P(V,V)$ and $P(H,H)$ for the state (1.7). Does it allows you to distinguish the state (1.7) from the Bell state (1.2)?

Q11 Show that $P(V_{45^\circ}, V_{45^\circ}) = (1+\cos(\phi))/4$. What is the difference with the Bell state?

To obtain a Bell state instead of the state (1.7), you need to compensate the dephasing ϕ, by using a Babinet compensator. If the axis of the compensator match the horizontal and the vertical direction, you can translate it orthogonally to the pump axis to linearly vary the dephasing between the two polarisation components (see figure 1.5). For the pump wavelength, this dephasing typically varies by 2π for a translation of about $5\,\mathrm{mm}$.

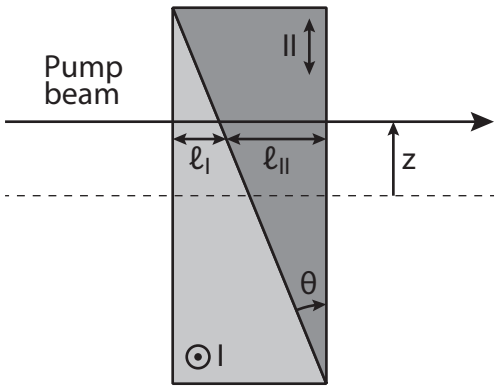

Figure 1.5 – The Babinet compensator consist in two pieces of uniaxial birefringent crystal. The pieces are beveled and mounted one against the other, in such a way that the optical axis of the two crystals are orthogonal (and both parallel to the entrance plane). If we note n_1 the refractive index along the optical axis, and n_2 the refractive index along the direction orthogonal to the optical axis, we see that the dephasing $\phi_{\text{B}} = \phi_H - \phi_V$ accumulated between the polarisation components of a beam with a wavelength λ is given by $\lambda\phi_{\text{B}}/2\pi = (n_2\ell_{\text{I}} + n_1\ell_{\text{II}}) - (n_1\ell_{\text{I}} + n_2\ell_{\text{II}}) = 2(n_2 - n_1)\tan(\theta)\, z$.

$\rightsquigarrow$ Mount the compensator on the bench.

$\rightsquigarrow$ Check that the coincidence rate are still equal when the analyzers are parallel horizontally and vertically. If it is not the case, it means that the axis of the compensator do not match the vertical and horizontal directions, and you need to slightly rotate the compensator.

$\rightsquigarrow$ Put the analyzers at 45° on both channels and plot the coincidence rate as a function of the compensator translation over $10\,\mathrm{mm}$ (by step of $0{,}5\,\mathrm{mm}$). Take an integration time of $10\,\mathrm{s}$.

Q12 Does the curve behave as expected? Comment on the contrast.

Q13 What are the points of the curve corresponding to a compensation of the dephasing induced by the crystals?

3.11 Variation of the join probability

The two theories we want to test (quantum theory and local hidden variable theory) do not predict the same variation of the join probability $P(V_\alpha, V_\beta)$ as a function of the relative angle $\alpha - \beta$. So it is interesting to measure it. Experimentally, we can estimate the probability $P(V_\alpha, V_\beta)$ by setting the analyzers at α and β and calculating the ratio between the coincidence rate and the photon rate on each channel.

Important note: Only complete the measurement below if you have enough time left before the end of the session. Otherwise, go directly to the Bell parameter measurement.

$\rightsquigarrow$ Fix the angle of one of the two analyzers at $0°$ and plot the variation of the coincidence rate as a function of the angle of the second analyzer. During this measurement, check that the photon rate on each channel remains approximatively constant. Re-do the same measurement, but this time set the first angle to $45°$.

Q14 Compare those measurements to the prediction of quantum mechanics (question **P6**).

3.12 Measure of the Bell parameter

You will now experimentally evaluate the Bell parameter defined by the relation (1.6), and whose value allows you to invalidate the local hidden variable theory. To do so, you will measure the join probabilities $P(V_\alpha, V_\beta)$, $P(H_\alpha, H_\beta)$, $P(V_\alpha, H_\beta)$ and $P(H_\alpha, V_\beta)$ for the following set of angles of analysis: $\{\alpha, \beta\}$, $\{\alpha, \beta'\}$, $\{\alpha', \beta\}$ and $\{\alpha', \beta'\}$ define on figure 1.2. To minimize the uncertainty of each measurement, one need to maximize the number of coincidences detected, so one needs to count them over a longer duration. Indeed, the fluctuations in the number of coincidences N_c detected over an interval T are linked to the photonic "shot noise", which has a Poisson statistics. This implies that the statistical uncertainty (standard deviation) $\sigma[n_\mathrm{c}]$ on the coincidence rate $n_\mathrm{c} = \langle N_\mathrm{c}\rangle / T$ verifies :

$$\sigma[n_\mathrm{c}] = \frac{\sigma(N_\mathrm{c})}{T} = \frac{\sqrt{\langle N_\mathrm{c}\rangle}}{T} = \sqrt{\frac{n_\mathrm{c}}{T}}\,, \tag{1.8}$$

so that the relative uncertainty

$$\frac{\sigma[n_\mathrm{c}]}{n_\mathrm{c}} = \frac{1}{\sqrt{\langle N_\mathrm{c}\rangle}} = \frac{1}{\sqrt{n_\mathrm{c} T}}\,. \tag{1.9}$$

Q15 If you count an average of $100\,\mathrm{coincidences/s}$, what is the standard deviation of the coincidence rate? What is the duration required to divide this standard deviation by 10?

$\rightsquigarrow$ Fill the Excel chart on the computer for each of the 16 measurements. Take an integration time of 10 or $20\,\mathrm{s}$ to have a good precision. The Bell parameter is then automatically calculated.

Q16 What value of the Bell parameter do you obtain and what are the error bars? Does your measurement allow you to invalidate the local hidden variable theory or the quantum theory?

Q17 What result would allow you to invalidate quantum mechanics?

P 2

Saturated absorption Sub-Doppler spectroscopy

Contents

At room temperature, the main cause of the broadening of atomic transitions in a gas is the Doppler effect. Saturated absorption spectroscopy, developed in the 1970s, makes it possible to overcome this broadening and resolve the hyperfine structure of atomic transitions. The aim of the practical work is to carry out saturated absorption spectroscopy of the D1 line of rubidium in order to observe its hyperfine structure. The source used is a laser diode tunable in wavelength around 795 nm.

1 Preliminary study

1.1 Doppler broadening

We consider an atomic gas of two-level atoms and denote ν_0 the frequency of the atomic transition. Doppler broadening, which is largely predominant at room temperature, results from the dispersion of the velocities of the atoms in the gas. The gas is illuminated by a laser beam of frequency ν propagating along the axis Oz in the positive direction. Among the atoms, only those whose V_z projection of the velocity along Oz satisfies the relation

$$\nu_0 = \nu\,(1 - V_z/c) \tag{2.1}$$

are in resonance with the wave and can absorb and re-emit light (c is the speed of light). Thus, if we sweep the laser frequency, **we obtain an absorption line profile that reflects the distribution of atomic velocities in the direction of the laser beam**.

P1 Quickly explain the demonstration of the formula (2.1).

Statistical physics shows that the velocity distribution of atoms in a perfect gas follows the Maxwell-Boltzmann law:

$$f(V_z) = \left(\frac{m}{2\pi \mathrm{k_B} T}\right)^{1/2} \exp\left(\frac{-mV_z^2}{2\mathrm{k_B} T}\right). \tag{2.2}$$

In this equation, V_z is the velocity along the z axis, T is the temperature of the gas, m is the mass of the atoms ($1.41\ 10^{-25}\,\mathrm{kg}$ for rubidium) and $\mathrm{k_B}$ is Boltzmann's constant ($1.38\ 10^{-23}\,\mathrm{J/K}$).

P2 Show that the width at half-height of the line broadened by the Doppler effect is :

$$\Delta\nu = \sqrt{8\ln 2}\sqrt{\frac{\mathrm{k_B} T}{m}}\frac{\nu_0}{c}\,. \tag{2.3}$$

P3 Use the formula 2.3 to calculate the Doppler broadening at $T = 20^\circ$ of the rubidium D1 line (centred at $795\,\mathrm{nm}$).

1.2 Structure of the rubidium D1 line

The rubidium cell you are going to use contains the two stable isotopes of the atomic species in the proportions of their natural abundance: 72% rubidium 85 and 28% rubidium 87. The wavelength of study ($795\,\mathrm{nm}$) corresponds to the transition from the fundamental level $5\mathrm{S}_{1/2}$ to the excited level $5\mathrm{P}_{1/2}$. The hyperfine structure is detailed in figure 2.1 for both isotopes.

P4 How many lines should we theoretically observe? Arrange these lines in ascending order of resonance frequency.

P5 Taking Doppler broadening into account, which lines can be resolved with a simple absorption spectrum? At what temperature would we need to go down to resolve the entire hyperfine structure? Knowing that the natural width of the excited levels is $6\,\mathrm{MHz}$, at what temperature would we have to go down to be able to measure it? How can this be achieved?

1.3 Saturation of absorption

Let's now return to a two-level gas of atoms. In general terms, the absorption $\mathcal{A}$ (in $\mathrm{cm^{-1}}$) of a laser beam of frequency equal to the atomic transition frequency is given by the effective resonance scattering cross-section σ_0 (in $\mathrm{cm^2}$) weighted by the difference between the densities of atoms in the fundamental level, n_1, and in the excited level, n_2 (in $\mathrm{cm^{-3}}$). This difference in density depends on the intensity I (in $\mathrm{W.cm^{-2}}$) of the laser beam and therefore on the

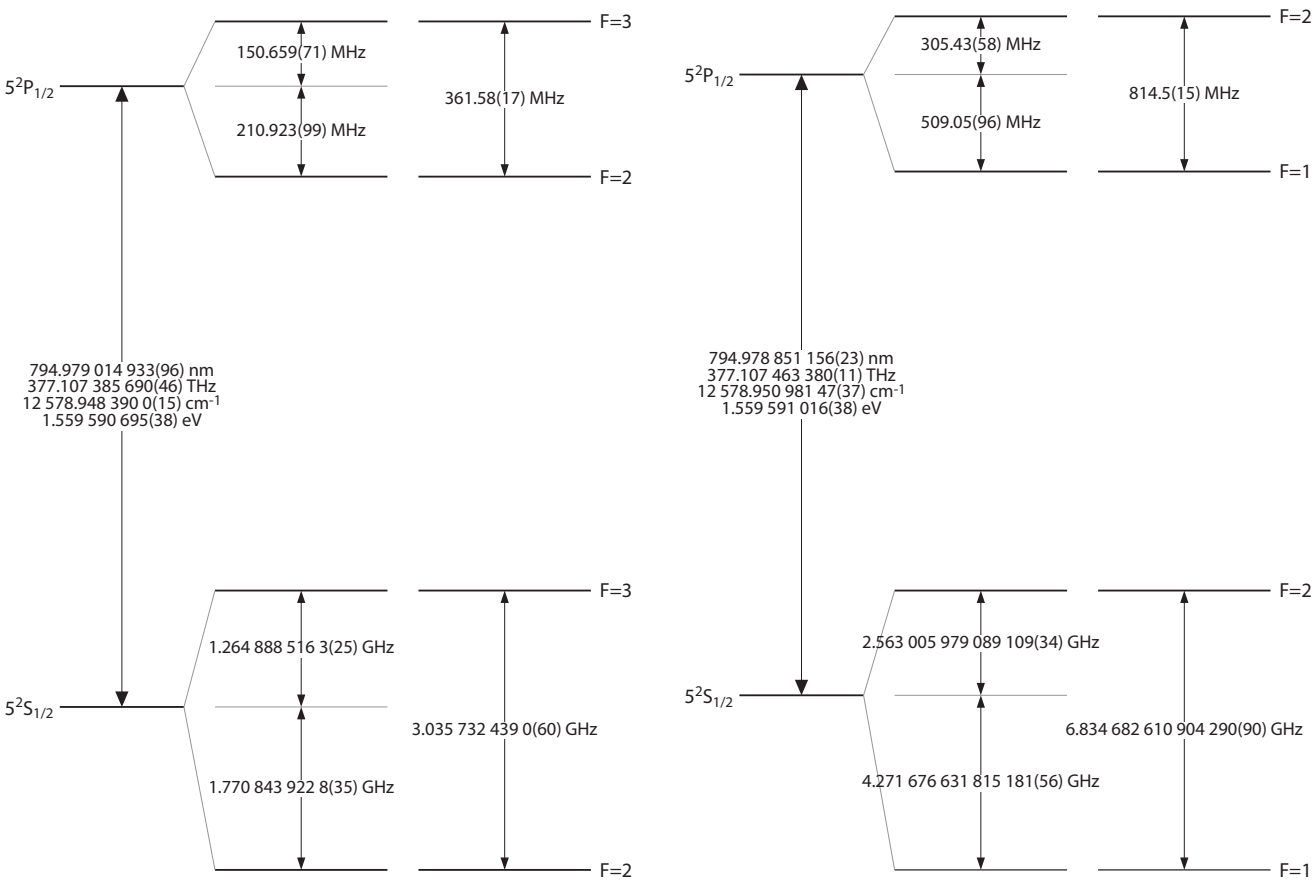

(a) Rubidium 85 **(b)** Rubidium 87

Figure 2.1 – Hyperfine structure of the D1 line of the two rubidium isotopes. The figure is taken from: Daniel A. Steck, *Rubidium D Line Data*, available online at http://steck.us/alkalidata.

absorption $\mathcal{A}$. This process of circular dependence ($\mathcal{A}$ depends on $n_1 - n_2$, which depends on I, which depends on $\mathcal{A}$) gives rise to the phenomenon of absorption saturation. In concrete terms, we show that:

$$\mathcal{A} = \sigma_0 \times (n_1 - n_2) \quad \text{avec} \quad n_1 - n_2 = \frac{n_\text{t}}{1 + I/I_\text{sat}} \,, \tag{2.4}$$

where n_t is the total density of atoms and I_sat is an intensity characteristic of the transition, called the **saturation intensity**, which is $1.6\,\text{mW/cm}^2$ for the atomic transition under consideration. The ratio $s = I/I_\text{sat}$, which is used in the equation 2.4, is called the **saturation parameter**.

P6 Make a qualitative comparison of the absorption in the limiting cases $s = I/I_\text{sat} \ll 1$ and $s = I/I_\text{sat} \gg 1$. What about absorption in the case of high intensity ($s \gg 1$). **This phenomenon is called absorption saturation**.

P7 Give the limit of the populations n_1 and n_2 in the case of strong saturation. Give an interpretation of absorption saturation by considering the evolution of the spontaneous emission

rate as a function of intensity.

P8 Is it possible to invert the populations on a 2-level system? Explain why.

1.4 Application to sub-Doppler spectroscopy (pump-probe method)

Consider two laser beams of the same frequency ν and counter-propagating (superimposed but propagating in opposite directions). The first beam, called the pump beam, propagates in the positive direction of the Oz axis and has sufficient intensity to saturate the absorption on the transition in question. The second beam, called the probe beam, propagates in the negative direction of the Oz axis and has too low an intensity to saturate the transition on its own. We are interested here in the absorption of the probe beam in the presence of the pump beam when their frequency is varied around the frequency of the atomic transition.

According to equation 2.1, for a given frequency ν, the atoms which absorb the pump are those for which $V_z = -c\,(1 - \nu/\nu_0)$ and the atoms which absorb the probe are those for which $V_z = +c\,(1 - \nu/\nu_0)$. There are then two cases, represented in figure 2.2 :

- if $\nu \neq \nu_0$, the atoms which absorb the pump and those which absorb the probe belong to different velocity classes. In this case, the presence of the pump has no effect on the absorption of the probe;
- if $\nu = \nu_0$, the same atoms absorb the pump and the probe, i.e. atoms with zero velocity along z ($V_z = 0$). As the pump is sufficiently intense to saturate the absorption, the probe is absorbed very little (absportion is reduced) at this precise frequency $\nu = \nu_0$.

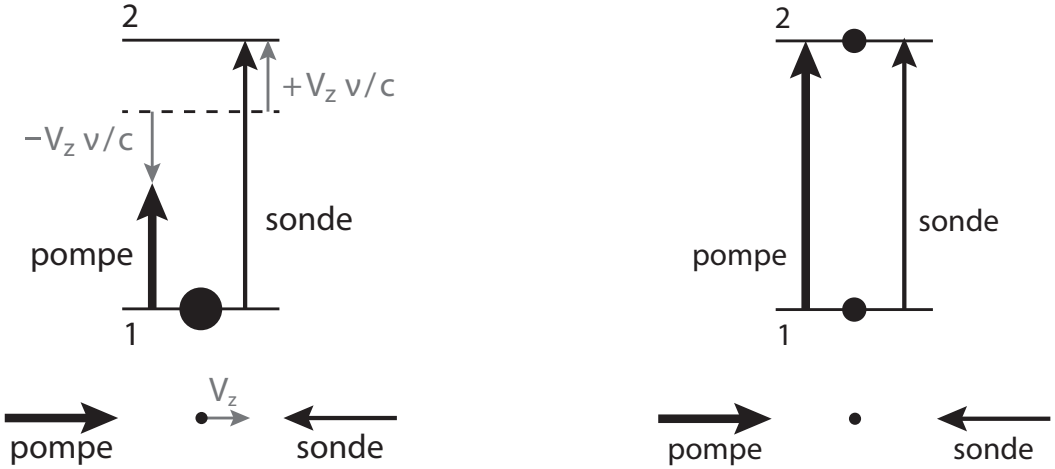

(a) $\nu < \nu_0$ **(b)** $\nu = \nu_0$

Figure 2.2 – Influence of the Doppler effect in the pump-probe configuration.

The absorption line profile of the probe therefore has a dual structure, with a narrow peak centred on the frequency of the atomic transition superimposed on the profile broadened by the Doppler effect. As you will see in the course of the labwork, the resolution offered by pump-probe spectroscopy is such that it can reveal the hyperfine structure of the atomic transition. Each transition then appears as a distinct peak in the Doppler profile, as shown in Figure 2.3.

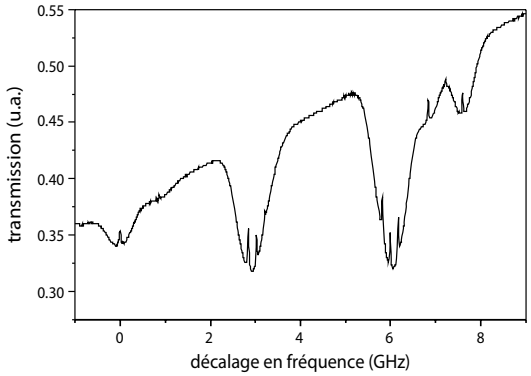

Figure 2.3 – Absorption spectrum around $795\,\mathrm{nm}$ obtained by the pump-probe method. The lines of the hyperfine structure appear as narrow peaks against a background broadened by the Doppler effect. The figure is adapted from: Svenja A. Knappe *et al.*, *Microfabricated saturated absorption laser spectrometer*, Optics Express **15**, 6293–6299 (2007).

P9 What is the intrinsic width of the saturated absorption peak? What are the reasons why this peak might appear wider?

2 Experimental realization

Precautions for using the laser diode Never disconnect the cables connecting the laser diode to its power supply. **The maximum power delivered by the diode is of the order of 30 to 50 mW, which is enough to cause irreversible eye damage in direct vision**. As the eye is not very sensitive to this wavelength, the beam can reach you without you noticing. So be careful not to put your eyes at bench level. Remove or hide any reflective objects that may be at beam level (watches, bracelets, rings, chains, bracelets, belt buckles, etc.). Check that all optical elements are firmly attached to the board when the diode is transmitting. Finally, use the laser safety glasses provided at the entrance to the room.

General precautions All the optical elements used are fragile, expensive and difficult to obtain (particularly the cell containing the rubidium). You will be making difficult adjustments, in the dark, and with a near-infrared viewfinder (which is not very convenient). So move the elements carefully, clamp the feet carefully after each modification and don't leave anything lying around the edge of the board.

2.1 Laser diode

The tunable laser used here is a "DBR" (Distributed Bragg Reflector) laser diode, which provides single-mode operation at a very fine instantaneous laser linewidth (around MHz, i.e. around $2\ 10^{-6}\,\mathrm{nm}$!!). However, fluctuations in current and temperature will introduce fluctuations in this frequency and cause it to broaden. In practice, the actual frequency linewidth is therefore higher, of the order of a few tens of MHz.

The laser diode package includes an optical fiber to prevent perturbing backward light reflection into the cavity [1], and the light is directly injected into a single mode polarizing maintaining optical fiber.

The laser emission frequency is a function of two parameters: the equilibrium temperature T_{eq} of the junction and the intensity i of the diode injection current. The emission frequency increases with T_{eq} and decreases with i (the wavelength increases with the current). In this labwork, we will vary the emission frequency using the current alone. The full characteristics of the laser diode used are detailed in the document at your disposal.

Temperature controller The junction equilibrium temperature is measured by a thermistor. The set temperature is fixed by a resistance value. Its value is preset so that the entire spectrum around line D1 can be observed by sweeping the current alone. **In principle, you will not need to change this setting**. If, however, you need to change the set temperature, to move away from a mode jump for example, be careful to do so only in very small steps. A sudden change would take you too far away from resonance and it would be difficult to find it again afterwards.

Current supply By default, set the current to around $120\,\text{mA}$ so that you can view the beam using the infra-red card (or simply on a piece of paper).

P10 If you want to see all the transitions in the rubidium D1 line for both isotopes, over what range should you vary the current in the laser diode?

P11 Compare the spectral width of the laser with the natural width of the atomic transition. Which of these two widths will determine the width of the absorption lines observed once the Doppler effect has been eliminated?

2.2 Fluorescence and absorption spectra

$\rightsquigarrow$ Place the cell in the path of the laser beam and adjust the observation camera so that the inside of the cell is clearly visible.

$\rightsquigarrow$ In total darkness, slowly vary the value of the current. In this way, you should be able to observe the fluorescence of the rubidium in the D1 line using the camera: the path of the laser beam shines in the cell for a precise value of current!

[1] Laser diodes are very sensitive to reflections (even very weak ones) from the beam towards the cavity, which can introduce significant fluctuations in the emission length. It is therefore necessary to use an optical isolator. This blocks the reverse return of light by using a Faraday rotator placed between two polarisers. The Faraday rotator used rotates a 45° rectilinear polarisation in the same direction regardless of the direction in which the light travels, so that if the polarisers are oriented to allow light propagating in one direction to pass, they will necessarily block light propagating in the other direction.

⇝ Once you have obtained fluorescence, complete the set-up described in figure 2.4. To visualise the lines of the two isotopes contained in the cell, sweep the diode's emission frequency by modulating the driving current with a triangular signal.

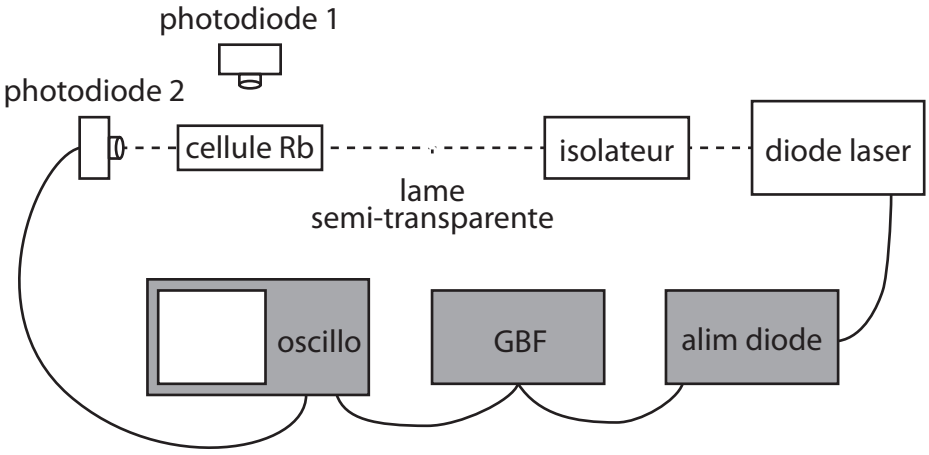

Figure 2.4 – Schéma du montage à réaliser pour observer les spectres de fluorescence et d'absorption.

⇝ Switch on the GBF and set it to produce a low-amplitude triangular signal at a frequency of around 10 Hz. Display the GBF signal on one of the oscilloscope channels.

⇝ Place one of the two photodiodes carefully against the cell (without contact), perpendicular to the laser beam, to capture part of the fluorescence signal. Monitor the photodiode signal on the other channel of the oscilloscope (set the adjustable gain to maximum) .

⇝ Modify the amplitude of the modulation applied to see the different fluorescence lines expected. Improve the signal obtained (by averaging if necessary.

⇝ Save the displayed signals with an USB stick (or take a photo of the screen, after you've turned on "stop").

Q1 Identify the different lines on the oscillogram and briefly explain how you did this.

Q2 Calibrate the oscillogram using the largest gap between two lines as a reference. Measure and check the spacing and relative positions of the different lines. Check that the width of the lines corresponds to that expected from the Doppler effect (or at least is of the right order of magnitude).

⇝ Place the second photodiode behind the cell and display the absorption spectrum on the oscilloscope channel previously occupied by the GBF (the GBF is moved to the synchro input). **Caution: adjust the gain to make sure you don't saturate the signal coming out of the photodiode, which happens very quickly!**.

⇝ Observe the fluorescence and absorption spectra simultaneously.

⇝ Observe the changes in the absorption spectrum when a density is added before the cell.

⇝ Now observe what happens if you place the density after the cell, and compare it with the previous situation (density before the cell).

⇝ Using the power meter provided, **measure the values of the saturation parameter** $s = I/I_{\text{sat}}$ for the intensity incident on the cell (with or without density).

Q3 Explain why the phenomenon of absorption saturation is clearly demonstrated qualitatively.

2.3 Sub-Doppler spectroscopy of hyperfine levels

The pump-probe setup is shown in Figure 2.5. The pump and probe beams must be superimposed at the gas cell.

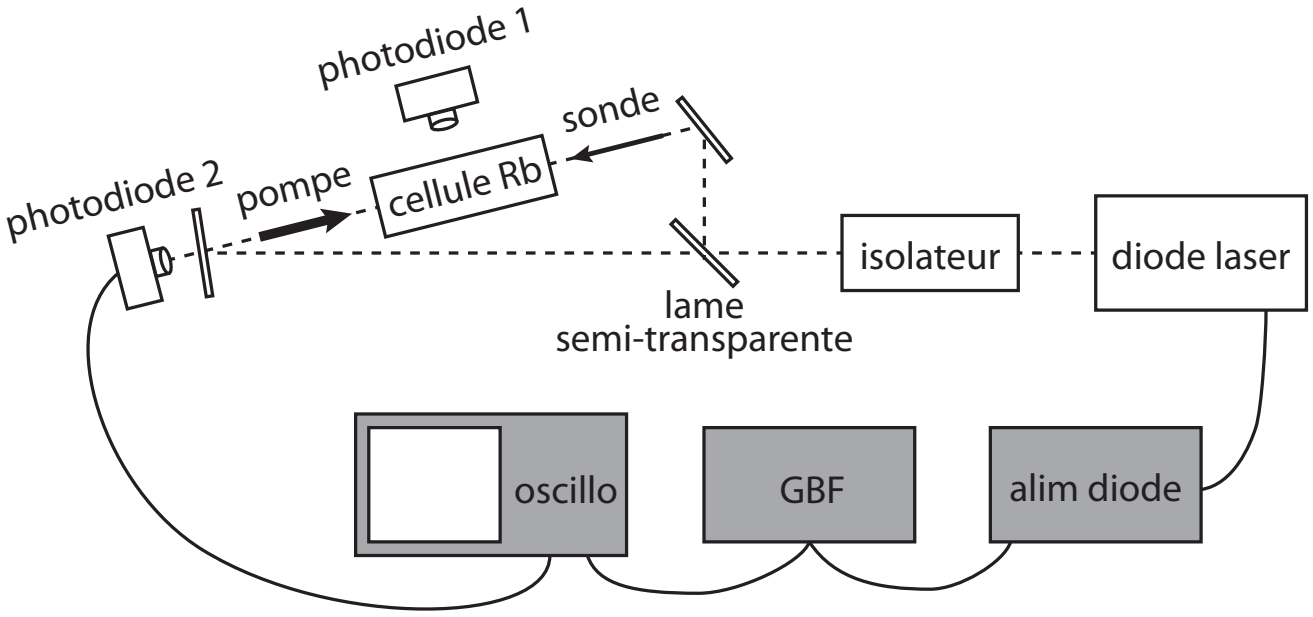

Figure 2.5 – Schéma du montage en configuration pompe-sonde.

⇝ Do not touch the power supply or GBF settings!

⇝ First place and adjust all the components, excluding the cell and photodiodes. Carefully superimpose the pump and probe beams, observing the laser spots on on separating plates with the infrared viewer.

$\rightsquigarrow$ Using the power meter, measure the values of the saturation parameter $s = I/I_{\text{sat}}$ for the pump and probe in this configuration.

$\rightsquigarrow$ Then position the cell and the photodiodes to visualise absorption on the probe beam and the fluorescence.

$\rightsquigarrow$ Save the displayed signals with an USB stick (or take a photo of the screen, after you've turned on "stop").

Q4 For the two isotopes, identify the lines of the hyperfine structure (using figure 2.1). Measure the relative positions of the hyperfine lines and compare the values obtained with the expected values. Also measure the width of the observed lines.

Q5 What do they correspond to?

In Doppler profiles covering two atomic transitions (as for rubidium 85), instead of 2 absorption lines you should observe 3 lines. The third line appears precisely in the middle of the 2 expected lines. This phenomenon is called crossover.

Q6 Explain the origin of the crossover line. To do this, repeat the reasoning given in section **??** for the case of an atom with two excited states.

Q7 Compare the absorption and fluorescence spectra. Is it possible to see the same saturation signature in the fluorescence spectra? Explain why.

P 3

Hong, Ou and Mandel experiment

1 Introduction

The Hong, Ou and Mandel (HOM) experiment, conducted in 1987 [1], is the first observation of a quantum interference between two photons with no classical explanation (*i.e.* no explanation with a wave description of light). This phenomenon appears when two indistinguishable photons arrive simultaneously at the two input ports of a 50/50 beam splitter. The distribution of the two photons between the two output ports of the beam splitter exhibit a surprising behavior, that can not be explained with a classical theory of light...

1.1 The HOM effect

If a photon arrives on a 50/50 beam splitter, it has 1/2 probability of being transmitted or reflected. When two photons arrive simultaneously on a beam splitter, each one at a different input (a or b), there are four possibilities (see figure 4.1) :

- The photon entered in a goes out in c, and the photon entered in b goes out in d;
- The photon entered in a goes out in d, and the photon entered in b goes out in c;
- Both photons go out in c ;
- Both photons go out in d.

[1] C. K. Hong, Z. Y. Ou et L. Mandel, *Measurement of subpicosecond time intervals between two photons by interference*, Physical Review Letters **59**, 2044 (1987)

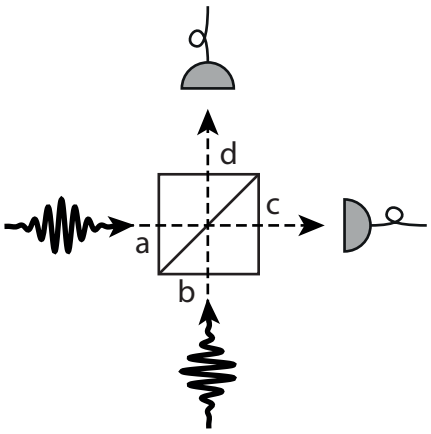

Figure 3.1 – Two indistiguishable photons arrive simultaneously on a beam splitter. Two single-photon detectors at the output c and d record which way the photons went out.

If the photons were classical particles, the 4 cases would always be equiprobable, in the case where the reflectivity and transmitivity of the beam splitter are equal. But according to the quantum theory, if the two particles are **indistinguishable** there is no way to know which particle is which at the output of the beam splitter, and therefore there is only 3 possible **observations** :

- we observe one photon in each output ;
- we observe two photons in output c ;
- we observe two photons in output d.

Then, according to quantum mechanics, the probability of observing a photon in each output results from the **interference** between the two **classical trajectories** $(a, b) \rightarrow (c, d)$ and $(a, b) \rightarrow (d, c)$. It then depends on the **relative phase** associated to those trajectories.

In our case, two photons are **indistinguishable** when their properties (polarization, frequency, transverse mode) can not be distinguished with our experimental setup. Note that the two photons do not need to be identical, which would imply that they have identical properties, for them to be indistinguishable. For instance, two photons with different frequencies (or energies) behave as indistinguishable photons as long as the experimental setup does not allow one to measure the difference in their frequencies. As a consequence, establishing whether two photons are indistinguishable or not depends on the experimental setup which is used.

1.2 Formalism

In classical electromagnetism, a beam splitter is modelled by a **real unitary matrix** , that links the **electrical fields** $\mathcal{E}_{a,b}$ of the inputs to the electrical fields $\mathcal{E}_{c,d}$ of the outputs:

$$\begin{pmatrix} \mathcal{E}_c \\ \mathcal{E}_d \end{pmatrix} = U \begin{pmatrix} \mathcal{E}_a \\ \mathcal{E}_b \end{pmatrix} \quad \text{with} \quad U = \begin{pmatrix} t & r \\ -r & t \end{pmatrix} . \tag{3.1}$$

The unitarity property $U^\dagger U = \mathbb{1}$ stands for the **energy conservation** between the input and the output of the beamsplitter. It leads to a relationship between the reflectivity and transmitivity coefficient of the beam splitter.

$$r^2 + t^2 = 1 \,. \tag{3.2}$$

A $50/50$ beam splitter corresponds to the case where $r = t = 1/\sqrt{2}$.

In quantum optics, the complex electromagnetic field is replaced by **creation and annihilation operators** :

$$\mathcal{E}_a \to \{\hat{a}, \hat{a}^\dagger\} \,,\ \mathcal{E}_b \to \{\hat{b}, \hat{b}^\dagger\} \,,\ \mathcal{E}_c \to \{\hat{c}, \hat{c}^\dagger\} \,,\ \mathcal{E}_d \to \{\hat{d}, \hat{d}^\dagger\} \,. \tag{3.3}$$

The beam splitter links those operators in the same way than with the electric fields :

$$\begin{pmatrix} \hat{c} \\ \hat{d} \end{pmatrix} = U \begin{pmatrix} \hat{a} \\ \hat{b} \end{pmatrix} \quad \text{and} \quad \begin{pmatrix} \hat{c}^\dagger \\ \hat{d}^\dagger \end{pmatrix} = U \begin{pmatrix} \hat{a}^\dagger \\ \hat{b}^\dagger \end{pmatrix} \,. \tag{3.4}$$

The unitarity property of the matrix U ensures that **the number of photons is conserved** between the input and the output :

$$\hat{c}^\dagger \hat{c} + \hat{d}^\dagger \hat{d} = \hat{a}^\dagger \hat{a} + \hat{b}^\dagger \hat{b} \,. \tag{3.5}$$

The quantum state that corresponds to a situation where two photons enter in a and b is obtained by using the operators $\hat{a}^\dagger$ and $\hat{b}^\dagger$ on the state which corresponds to the **electromagnetic vacuum** : $\hat{a}^\dagger \hat{b}^\dagger |\text{vacuum}\rangle$. By inverting the relation 3.4, one can link this input state to the output state:

$$\begin{aligned} \hat{a}^\dagger \hat{b}^\dagger |\text{vacuum}\rangle &= (t\hat{c}^\dagger - r\hat{d}^\dagger)(r\hat{c}^\dagger + t\hat{d}^\dagger)|\text{vacuum}\rangle \\ &= (tr\hat{c}^\dagger \hat{c}^\dagger + t^2 \hat{c}^\dagger \hat{d}^\dagger - r^2 \hat{d}^\dagger \hat{c}^\dagger - rt\hat{d}^\dagger \hat{d}^\dagger)|\text{vacuum}\rangle \,. \end{aligned} \tag{3.6}$$

In the case of a $50/50$ beam splitter, we can use the commutativity of the operators acting on the different modes of the electromagnetic field. The last expression then become:

$$\hat{a}^\dagger \hat{b}^\dagger |\text{vacuum}\rangle = \frac{1}{2}(\hat{c}^\dagger \hat{c}^\dagger - \hat{d}^\dagger \hat{d}^\dagger)|\text{vacuum}\rangle \,. \tag{3.7}$$

The interpretation of this equation is straightforward: at the output of the beam splitter, the states corresponding to the situation where two photons are at the output c or d are equiprobable, but the probability of having a photon on each output is zero. Therefore **we never observe any coincidence** between the detectors c and d.

2 Experimental realization

2.1 Description of the experimental setup

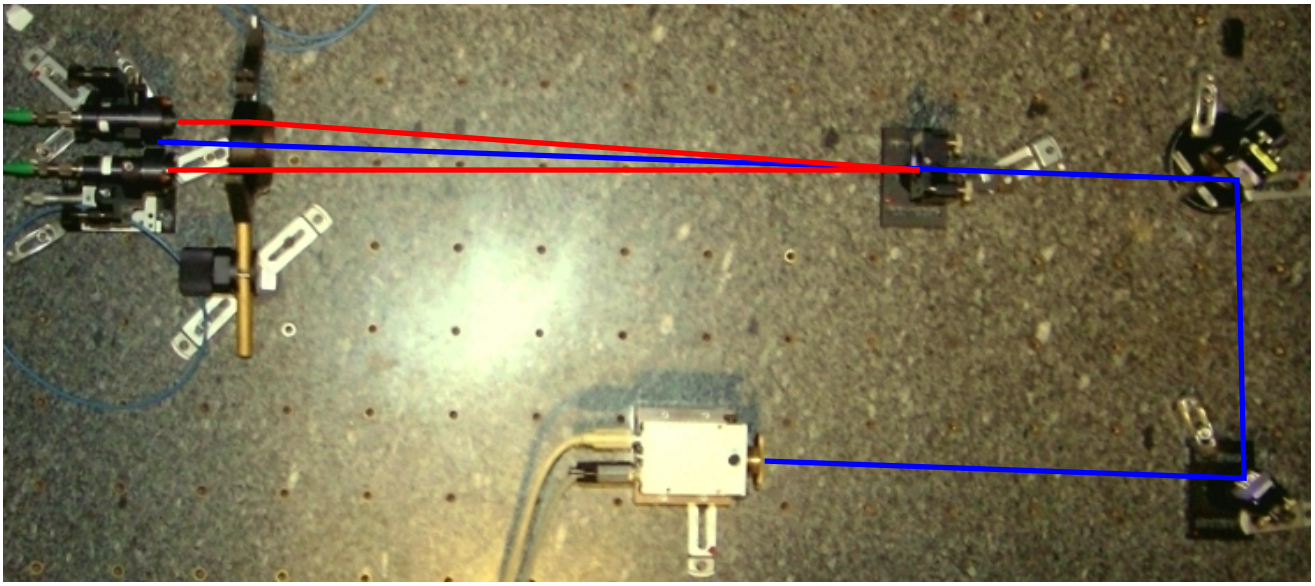

Figure 3.2 – View from above. We see the laser diode, two mirrors to set the alignement, the non-linear crystal, the optics for the conjugation and two fibered collimators. The optical path of the pump beam and the photons pairs are sketched.

To observe the HOM effect, one needs to create pairs of indistinguishable photons and send them into a beam splitter (see figure 3.2). To do so, we will use a parametric down-conversion process inside a $\chi^{(2)}$ non-linear crystal (BBO) than can convert a pump photon at $\lambda_p = 405\,\mathrm{nm}$ into a pair of photons at $2\lambda_p = 810\,\mathrm{nm}$. The twin photons are emitted symmetrically with respect to the pump axis, within a cone of about $3°$ of aperture. The pump beam, emitted from a laser diode, is horizontally polarized. The twin photons created in this process, are vertically polarized.

The twin photons are then injected inside two polarization-maintaining monomode fibers, thanks to a pair of fibered collimators and an optical doublet, whose focal point is set inside the crystal. An interferometric filter at $810\,\mathrm{nm}$ allows us to get rid of most of the stray lights. The fibered light then enters inside a module made of two waveguides that will play the role of the beam splitter. The waveguides are mounted very close to each other so that the transverse mode of the light propagating in each waveguide overlap the other one. The fibers are connected to a detection module using Avalanche PhotoDiodes (APD). A FPGA card is used to count the number of detected photons in each output. A simultaneous detection on each output is counted as a **coincidence**. A Labview code is then used to display the number of events and coincidences.

2.2 Single photon detection module

The single photon detection module is an exceptional tool, adapted for this kind of experiment. It is made of four fibered channels, linked to four APDs. On each channel, the detection of a photon triggers the emission of a $25\,\mathrm{ns}$ TTL pulse ($0\,\mathrm{V}$ to $5\,\mathrm{V}$). We will just use two channels out of four for this experiment, labeled A and B.

Warning ! Those detectors are very, very expensive and would be destroyed by a strong photon flux! Always check that the interferometric filters are installed to protect the photodiodes. Wait for the teacher authorization to switch on the detectors, and make sure that the main lights are off and the door is closed.

2.3 Event and Coincidence counter

The FPGA card counts the TTL pulses emitted by the detectors (after a conversion from $0\,\mathrm{V}$ to $5\,\mathrm{V}$ to $0\,\mathrm{V}$ to $3{,}3\,\mathrm{V}$), and the number of coincidences between the A and B pulses within an adjustable integration time. To count the coincidences, the FPGA card proceeds as follows: when a pulse arrives on channel A, a time window of adjustable duration is open; if a pulse arrives on channel B before this window is closed, a coincidence is counted. The card send the counting information to the computer via a RS232 link, and the informations are displayed by a Labview code. All the connections are already done, and we payed attention to the fact that the cables linking the APD to the coincidence counters have the same length.

Q1 Why do the cables need to have the same length?

$\rightsquigarrow$ Perform the following settings and measurements:

- Before doing anything else, switch on the FPGA card, then start the Labview program.
- Switch off every lights and turn the photons counters on.
- Measure the number of dark counts. The lower this number, the better the detectors are.
- Switch on a distant light and check that the number of detected photons stays way below $10^6\,\mathrm{photons/s}$.

2.4 Number of accidental coincidences.

For now, since the light sources are chaotic, the photons arriving in A and B are not correlated, and therefore the coincidences are accidental. We note n_A and n_B the **counting rate** (average number of photons per second) on channels A and B, n_f the rate of accidental coincidence, and τ, the duration of the coincidence window.

Q2 *Show that the rate of accidental coincidence is given by :* $n_f = n_A\, n_B\, \tau$.

The last two switches of the FPGA card, SW16 and SW17, allow one to choose the duration of the coincidence window (see table 3.1). The numbers given in this table are approximate and must need be measured.

SW16	SW17	τ (ns)
off	off	~ 70
on	off	~ 20
off	on	~ 14
on	on	~ 7

Table 3.1 – Duration of the coincidence window.

$\rightsquigarrow$ Measure the rate of accidental coincidences for each of the four configurations and calculate the durations of the four coincidence windows using the formula established in question 2.

This measure allows one to check the behavior of the coincidence counters. Call the teacher if the results are different from the value of table 3.1.

2.5 Pump diode

The pump diode is a $405\,\mathrm{nm}$ laser with about $60\,\mathrm{mW}$ of output power. The light emitted by the diode is linearly polarized. The wearing of security glasses is mandatory!

$\rightsquigarrow$ Make the following settings:

- Press the two buttons to turn on the temperature regulator of the diode. The temperature is already set to obtain the correct wavelength. Don't try to change it.
- Press the two buttons to turn on the current supply of the diode, and set the current at maximum (about $95\,\mathrm{mA}$).
- Briefly check the alignement of the beams (they should be already well aligned).

2.6 Parametric conversion

The photons pairs are produced by parametric down conversion in non-linear crystals β-BaB2O4 (baryum β-borate, BBO for short). During the non-linear process, a photon of the $405\,\mathrm{nm}$ pump can be converted in a pair of twin $810\,\mathrm{nm}$ photons. Recall that the two photons of the pair may have slightly different energies (or wavelenghts) since only their sum is set by the energy of a $405\,\mathrm{nm}$ pump photon (energy conservation in the process of parametric down conversion).

The BBO is a negative uniaxial birefringent crystal. We use a type I phase matching, meaning that the twin photons have the same polarization.

Q3 Recall what are the two conditions satisfied by a non-linear process. Which one is called the phase matching condition?

The pump beam is orthogonal to the entrance plane of the crystal. The optical axis of the crystal and the axis of the pump are forming an horizontal plane (see figure 3.3).

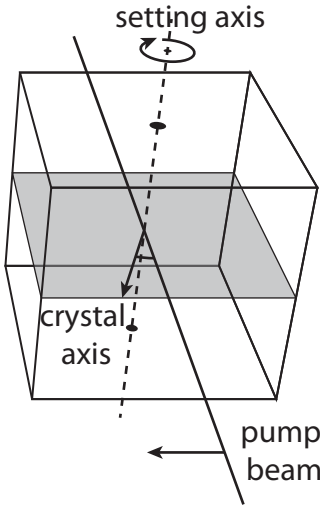

Figure 3.3 – Orientation of the optical axis of the crystal with respect to the pump axis.

The pump is horizontally (extraordinary) polarized and the $810\,\mathrm{nm}$ twin photons emitted from the crystal are vertically (ordinary) polarized. The refractive indexes n_o and n_e which characterize respectively the crystal axis and the orthogonal axis are given in table 3.2. From those indexes, one can calculate the index n_θ seen by the pump while it propagates through the crystal:

$$1/n_\theta^2 = \sin^2(\theta)/n_o^2 + \cos^2(\theta)/n_e^2\,. \tag{3.8}$$

θ being the angle between the propagation axis and the crystal axis (see figure 3.3).

wavelength (nm)	n_o	n_e
405	$1{,}691\,835$	$1{,}567\,071$
810	$1{,}660\,100$	$1{,}544\,019$

Table 3.2 – Refractive index of the BBO crystal along its optical axis, at a temperature of $293\,\mathrm{K}$.

Q4 Using a spreadsheet (Excel), calculate $n_\mathrm{e}(405,\theta)$ as a function of θ in the near range of $\theta = 30^\circ$. For what precise angle θ is type I collinear phase tuning achieved?

If we deviate slightly from this precise θ angle by modifying the crystal's inclination, we'll still obtain a type I, but non-collinear, phase tuning.

Q5 The collimators are positioned in such a way that they are forming with the crystal an isosceles triangle, with a 3° aperture. What should be the angle θ for the twin photons to be correctly collected by the collimators?

2.7 Settings of the collimators

The optical fibers are polarization-maintaining fibers. Their own axis are parallel to the horizontal and vertical axis. One of the own axis can be spotted thanks to a tip on the connector.

Q6 Why are those polarization-maintaining fibers crucial to observe the HOM effect?

Now you need to image the area of emission of the photons pairs onto the core of each fibers, by tuning the orientation of the collimators. This is a difficult setting because the fibers' cores have a diameter of $5\,\mu\mathrm{m}$ only. A trick is to make light propagates in the other direction (from the collimators to the crystal) by injecting a $670\,\mathrm{nm}$ auxiliary laser at the output of the polarization-maintaining fibers. You then have two beams coming out of the collimator. Focalise them inside the crystal and superimpose them to the pump beam. Of course you need to take the filter away from the collimator because they would cut the $670\,\mathrm{nm}$ light. Don not forget to put them back before switching the photon counters on again.

Warning ! You must switch the single photon detection module off every time the fibers are disconnected, and every time the filter are taken away from the collimators. Don not forget to put them back before switching the photon counters on again. Always protect the fibers' extremity with a cap.

Even with this method, it is difficult to inject the fibers. You will have to be very cautious (and probably try several times) to set the collimators correctly. However, as soon as you manage to inject a small fraction of the twin photons, the setting becomes a lot easier, you then just have to optimize the number of coincidences by fine-tuning the position of the collimators.

Remark The screws of the collimators' mounts are the only elements you need to touch during this setting. If you lose all the signal in the process (and you are not able to recover it) call the teacher.

$\rightsquigarrow$ Measure the coincidences rates.

Q7 Calculate the rate of accidental coincidences.

Q8 Do you need to account for them?

2.8 Observation of the HOM effect

Once the coincidence rate is high enough (about $600\,\mathrm{coincidences/s}$), you are ready to observe the HOM effect. One of the collimators is mounted on a translation stage. Record the number of coincidences as you gently move the translation stage (for instance by step of $10\,\mu\mathrm{m}$). To lower the uncertainty of your measurements, you need to raise the number of detected coincidences, so you need to count coincidences over a longer time interval. The fluctuations of the number of coincidences N_c measured during a time T is linked to the photonic shot noise, which follows a Poisson law. It means that the standard deviation $\sigma[n_\mathrm{c}]$ on the coincidence rate $n_\mathrm{c} = N_\mathrm{c}/T$ verifies :

$$\sigma[n_\mathrm{c}] = \frac{\sigma(N_\mathrm{c})}{T} = \frac{\sqrt{N_\mathrm{c}}}{T} = \sqrt{\frac{n_\mathrm{c}}{T}}\,., \tag{3.9}$$

which leads to the relative uncertainty :

$$\frac{\sigma[n_\mathrm{c}]}{n_\mathrm{c}} = \frac{1}{\sqrt{N_\mathrm{c}}} = \frac{1}{\sqrt{n_\mathrm{c}T}}\,. \tag{3.10}$$

Q9 Assuming you count an average of $100\,\mathrm{coincidences/s}$, what is the standard deviation on the coincidence rate? How long should the time interval be to reduce this deviation by a factor of 10?

In practice, you will count the coincidences during a time interval of 10 or $20\,\mathrm{s}$.

$\rightsquigarrow$ Plot the coincidence rate as a function of the position of the translation stage. Add the error bars on your graph.

Q10 Interpret the curve.

$\rightsquigarrow$ What is the depth of the dip?

Q11 Why does it not go to zero?

$\rightsquigarrow$ What is the the full width at half minimum of the dip?

Q12 Compair it to the coherence length of the $810\,\mathrm{nm}$ photons, which is given by the the filter ($10\,\mathrm{nm}$ width).

The width of the HOM dip is given by the energy difference of the twin photons created.

Q13 Explain why, using the notion of indistinguishability of the photons detected.

It is now possible to add interference filters of width $5\,\mathrm{nm}$.

Q14 What width of dip should we get in this case?

⇝ If you have time, add these filters in front of the $10\,\mathrm{nm}$ wide filters and repeat the HOM dip measurements.

⇝ Measure the new width of the HOM dip.

Q15 Compare it with the new energy difference of the photons detected using the $5\,\mathrm{nm}$ width filters.

P 4

NV center magnetometry

Contents

1 Pedagogical objectives

At the end of this labwork session, you'll be able to :

- use a method to a align a light beam ("walking the beam")
- measure the RF spectrum of NV centres
- analyze the RF spectrum of NV centers under an externally applmied magnetic field
- reconstruct a vectorial magnetic field from this RF spectrum
- describe a method to reconstruct weak magnetic fields such as the magnetic field of the Earth.

2 Introduction

An NV center is a crystalline defect of diamond. It's also known as a "colored center", because on a macroscopic scale, when these defects are present in very large numbers, they give diamond a colored hue. Since diamond is made up of a network of carbon atoms, the NV center consists of the substitution of one of these atoms by a nitrogen atom (N), directly adjacent to a vacancy (V). (see Fig. 4.1).

In the quantum world, electrons are described by a wave function. The wave functions of electrons around an atom are confined (because the electrons remain close to the nucleus). The confinement of this wave gives rise to the quantization of its energy states, in the same way that a wave (e.g. a light wave) sees its modes of propagation confined by the existence of boundary conditions, in a cavity or a waveguide.

In the case of NV centers, the disruption of the crystal lattice causes the wave function of certain electrons to be confined to the defect. It is therefore often said that an NV center behaves like an artificial atom: while crystalline diamond is a large-gap semiconductor, the defect introduces electronic energy levels within this gap.

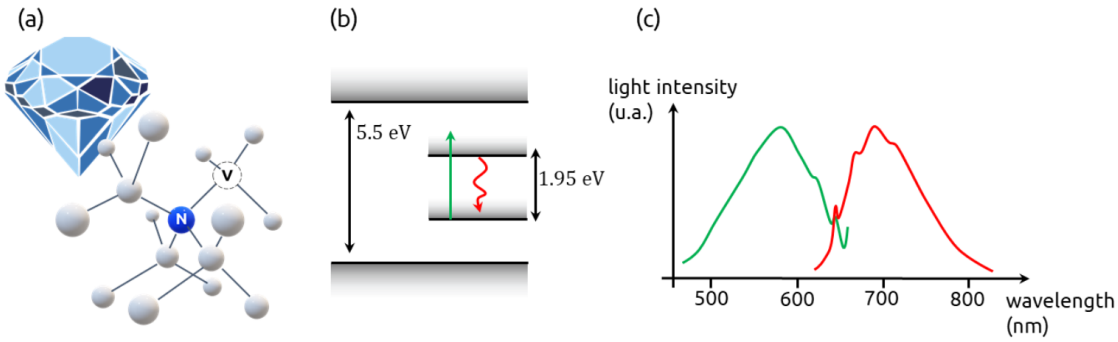

Figure 4.1 – Diamond NV center. (a) Schematic representation of an NV center, with a nitrogen atom (N) next to a vacancy (V).(b) Energy levels of diamond. Diamond is a wide-gap semiconductor. The presence of an NV center creates a sublevel within the gap.

The optical transition of the defect is at 637 nm. The interaction between this defect and the crystal, via phonons, causes a significant broadening of this transition. In practice, the absorption spectrum of the defect consists of a broad lobe centered around 550nm. Fluorescence at this level undergoes a Stokes shift, and takes the form of a broad lobe centered around 700nm, in the red part of the visible spectrum. Each lobe is around 200 nm wide.

Although NV centers are naturally present in diamond, it is possible to introduce NV centers in controlled densities into diamond samples (usually synthesized).

2.1 Defect geometry

Diamond is a crystal with a...diamond-like structure. It is a crystal with a blende structure, in which all sites are occupied by carbon atoms. It can be described as a face-centered cubic structure in which half the tetrahedral sites are occupied, two in the lower half of the cube describing the mesh, along a small diagonal, and two in the upper half, along the other small diagonal

.

The structure of an NV center is inscribed in this mesh, by substitution of one of the carbon atoms by a nitrogen, and creation of a gap by replacement of one of the surrounding carbon atoms.

The natural axis of symmetry of an NV center is the axis connecting the nitrogen atom to the gap. By construction, there are therefore 4 possible orientations of an NV center in a diamond crystal, corresponding to the 4 possible vacancy positions for a given nitrogen atom. (see Fig 4.2).

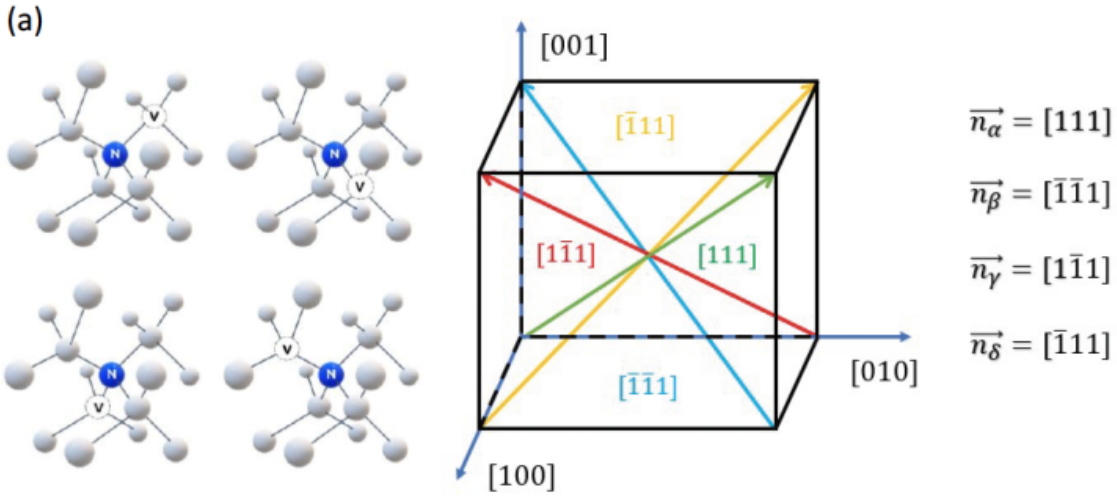

Figure 4.2 – The four possible orientations of NV centers in a solid diamond crystal and corresponding Miller notations.

3 Energy levels and spin

An NV center has a total spin $S = 1$. The fundamental level and the excited level of the optical transition of interest are therefore spin triplets: they are characterized by the quantum number m_S, which can take on the values 0,1, depending on the projection of the spin on the quantization axis (which is therefore the axis of the NV center). (see Fig 4.3).

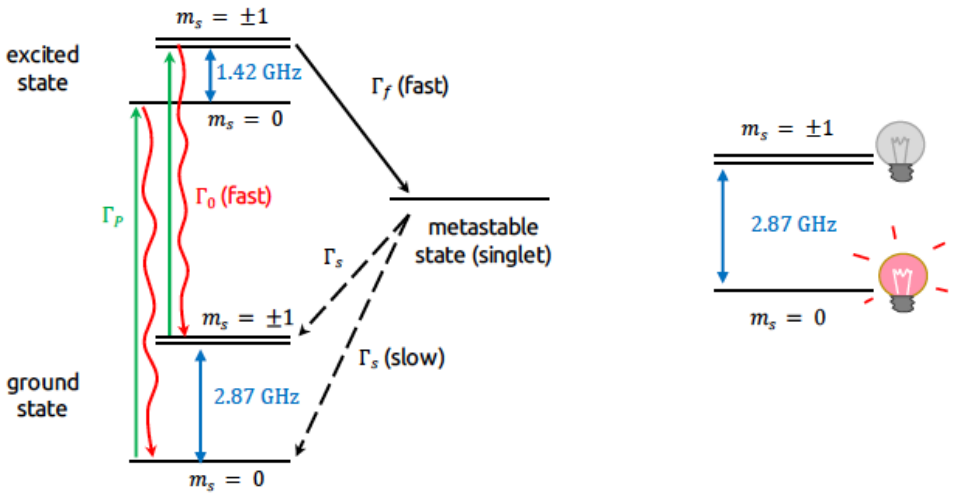

Figure 4.3 – Energy level structure of an NV center, comprising a triplet of ground states and a triplet of excited states

The energy degeneracy between the $|m_S = \pm 1\rangle$ and $|m_S = 0\rangle$ levels is partially overcome by spin-spin interaction. These two sets of levels are separated by an energy whose corresponding frequency is $D_f \approx 2.87\text{GHz}$ for the fundamental triplet and $D_e \approx 1.42\text{GHz}$ for the excited

triplet. It is therefore possible to use a laser to induce an optical transition from one of the fundamental levels to the excited state of the same spin; or to use a radio-frequency antenna to induce transitions within the same set of levels, either fundamental or excited.

A crucial point in the energy level structure of an NV center is the presence of a metastable singlet state. The excited state $|m_S = 0\rangle$ is not coupled to this metastable state and will always de-excite to the corresponding ground state by emitting a photon. For excited states $|m_S = \pm 1\rangle$, however, there is a probability of non-radiative de-excitation from the levels to the metastable state, i.e. without photon emission.

In other words, when the NV center is placed in the $|m_S = \pm 1\rangle$ states, it emits less fluorescence as it de-excites: this property is at the heart of the experiments that will be carried out during the course of the labwork.

3.1 Zeeman effect

The energy levels of the NV center are given by the Hamiltonian of the system. In the (X, Y, Z) basis related to the NV center, with the Z axis aligned with the NV center, this Hamiltonian is written :

$$\hat{H} = hD_f \hat{S_Z}^2 + hE(\hat{S_X}^2 - \hat{S_Y}^2) + g_{\mathrm{NV}}\mu_B \mathbf{B} \cdot \hat{\mathbf{S}} \tag{4.1}$$

where D_f is the zero-field separation factor of the fundamental levels discussed above, related to the spin-spin interaction, and is equal to $2.87GHz$; E is a splitting factor related to imperfections in the crystal lattice; μ_B is the Bohr magneton and g_{NV} is the Landé factor associated with the $\mathbf{S}$ spin of the NV centers. $\mathbf{S}$ represents the spin operator and its components, the Pauli spin matrices; $\mathbf{B}$ represents the external magnetic field that can be applied.

Under some approximations, the Hamiltonian can be simplified to contain only the contribution of the magnetic field aligned with the center NV :

$$\hat{H} \approx hD_f \hat{S_Z}^2 + g_{\mathrm{NV}}\mu_B B_{NV} S_Z + hE(\hat{S_X}^2 - \hat{S_Y}^2) \tag{4.2}$$

This Hamiltonian explains the degeneracy lift of the $ketm \pm 1$ levels: at zero field, the deformations of the crystal lattice give rise to a contribution linked to E; in addition, there is a splitting linked to the amplitude of the projection of the magnetic field onto the axis of the NV center: this is the Zeeman effect. The expression for the frequency splitting is then given by :

$$\Delta f_{\pm} = D \pm \sqrt{E^2 + (g_{NV}\mu_B BNV^2)} \tag{4.3}$$

Pour des champs suffisamment grands, le splitting Zeeman est donné par :

$$\Delta f_{\mathrm{Zeeman}} \approx 2g_{NV}\mu_B BNV \approx 56\mathrm{MHz/mT}.B_{NV} \tag{4.4}$$

3.2 Preliminary questions

The session consists in carrying out *Optically Detected Magnetic Resonance* (or ODMR) measurements. The protocol is as follows: the fluorescence of an NV center illuminated by a laser is detected. The NV center itself is placed on an RF antenna. The fluorescence intensity is observed by switching on the RF antenna and performing a frequency sweep around the transition between the $|m_S = 0\rangle$ and $|m_S = \pm 1\rangle$ states of the fundamental triplet.

P1. Schematically represent the ODMR spectrum of a single NV center at zero field (B=0), then at non-zero field.

P2 How does this ODMR spectrum measure the amplitude of a magnetic field component?

A diamond crystal can contain numerous NV centers, in 4 possible orientations. A fluorescence experiment thus simultaneously probes 4 different populations of NV centers, each associated with a different projection of the same magnetic field on the center's orientation, and thus presenting 4 different splitting values.

P3. Schematically represent the ODMR spectrum of a diamond crystal containing numerous centers at zero field, then at non-zero field.

4 Optical setup

WARNING!!!

In this TP, the maximum power of the 532 nm laser is 140 mW, i.e. over 100 times the eye's permanent damage threshold.

The orange box should never be opened when the laser is operating at a level above 1 percent. For any changes to the optical table, lower the laser power below 1 mW, then open the box(es) before adjusting.

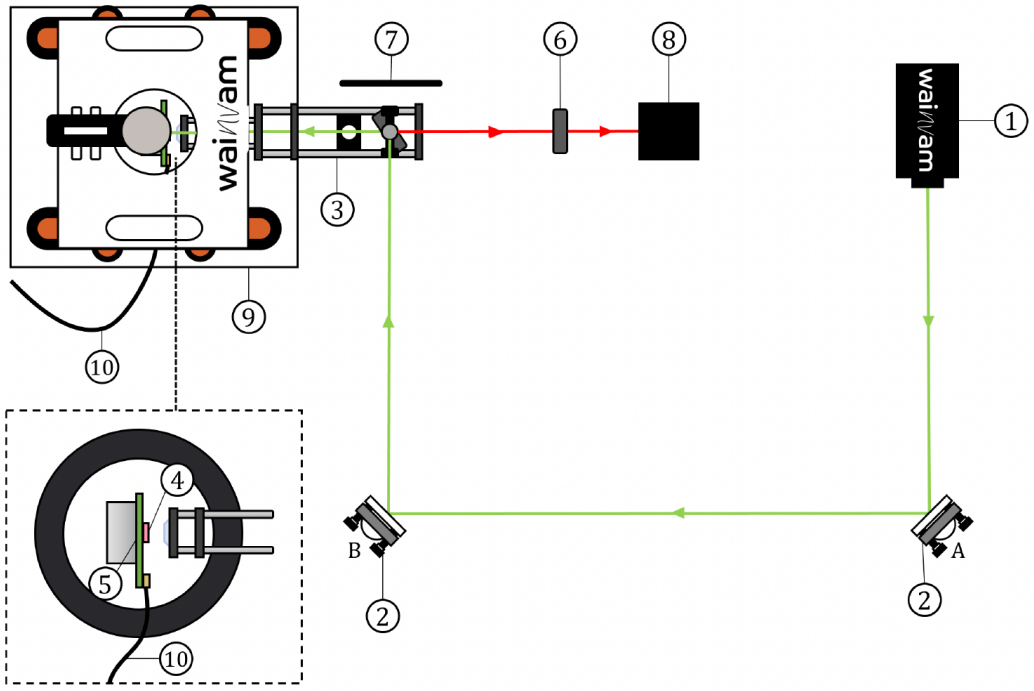

Figure 4.4 – Setum schematic 1 - Laser source. 2 - Alignment mirrors. 3 - Caged system comprising irises, dichroic mirror and aspherical focusing lens. 4 - NV-doped diamond sample. 5 - RF antenna, sample support. 6 - High-pass filter (lambda). 8 - Detector. 9 and 10 - Coils and their power supplies.

The optical set-up consists of a 532 nm laser, sent by two mirrors to a dichroic mirror, towards an asphere lens focusing the beam on a small diamond sample rich in NV centers, placed on an RF antenna, and in the middle of three pairs of coils allowing magnetic fields to be applied along the X, Y and Z axes (linked to the laboratory reference frame). The red fluorescence of the NV centers follows the opposite path, but is transmitted by the dichroic mirror, towards a photodiode.

The laser control signal and the photodiode signal can be controlled via the WAINTEACH control software.

5 Experiments

5.1 Aligning the beam ("beam walking")

Before starting measurements, we need to fine-tune the alignment of the laser on the sample. To do this, we adjust the micrometric screws on the two mirrors, so that the beam passes through two diaphragms, whose straight line joining the two centers defines the optical axis of the setup.

As the rest of the set-up has already been adjusted, it is not necessary (and not recommended) to touch other elements of the set-up. If you feel the need (or curiosity!) to do so, please call the teacher.

- Turn on the laser at the minimum power available (about 1 mW or 1 percent).
- Close the first diaphragm (closest to the source) until it is slightly smaller than the beam diameter.
- Use the mirror closest to the source to center the beam on this diaphragm.
- Open the first diaphragm fully, then close the second diaphragm (furthest from the source), again until it is slightly smaller than the beam diameter.
- Use the second mirror (furthest from the source) to center the beam on the second diaphragm.

You can repeat these steps several times to fine-tune the beam so that it passes through both diaphragms. You can now reopen both diaphragms.

You can then fine-tune the position of the mirrors by optimizing the fluorescence signal collected by the photodiode: as this signal is proportional to the laser power actually pumping the diamond sample, it can be used to further improve the alignment.

- Launch the software via the desktop shortcut and, in the window that opens, click on "load waintech".
- "Time Acquisition" tab lets you plot the photodiode signal as a function of time. Choose the number of points and the duration of signal acquisition, then click on "Start" to launch acquisition.
- Fine-tune the mirrors to optimize the signal received by the photodiode. With the laser intensity set to 1 percent (i.e. around 1 mW), and the photodiode placed in the dark (the box closed), you should obtain a signal of the order of $30mV$.

5.2 Zero field measurement

The aim of this first experiment is to carry out an ODMR measurement at zero field - without applying a magnetic field to the coils.

- With the boxes closed, turn up the laser power to 80 mW.
- Display the "ODMR Acquisition" tab of the Kwanteach software.
- Record a first ODMR spectrum, for example between 2.8 GHz and 2.94 GHz, at 5 dBm RF power.
- Save this acquisition (and subsequent ones) in the same folder, using the software's "save" function.

You can easily analyze the spectra you record using the dedicated graphical "Magnetometry GUI", accessible via a desktop shortcut. This interface lets you identify, by fitting experimental points, the value of the central frequency of certain patterns, the frequency width and the uncertainty associated with the fitting parameters.

- In the "*fit data*" tab, first select the .dat spectrum you wish to analyze. This should then be displayed in the dedicated window.
- Click on "*Update fit options*", then use the mouse (CTRL + click) to select the center of the peak you wish to fit.
- Once you've selected all the desired peaks, click on "perform fit" to start the adjustment. You'll then get the center frequency, "x0", and the peak's half-height width, "w0".

Q1. Note the center frequency corresponding to a drop in fluorescence. How do you explain this drop in fluorescence? What transition between levels in the NV center does this center frequency correspond to?

Q2. If you look carefully, or average over several acquisitions, you should see two peaks within the central peak. Which Hamiltonian term explains the physical origin of these two peaks? Comment.

Then bring the horseshoe magnet close to the sample (you could, for example, slide it between two horizontal coils). Repeat the spectrum measurement.

Q3. What do you observe? Describe the changes observed and explain qualitatively why the shape of the ODMR spectrum has changed.

5.3 Influence of the field orientation

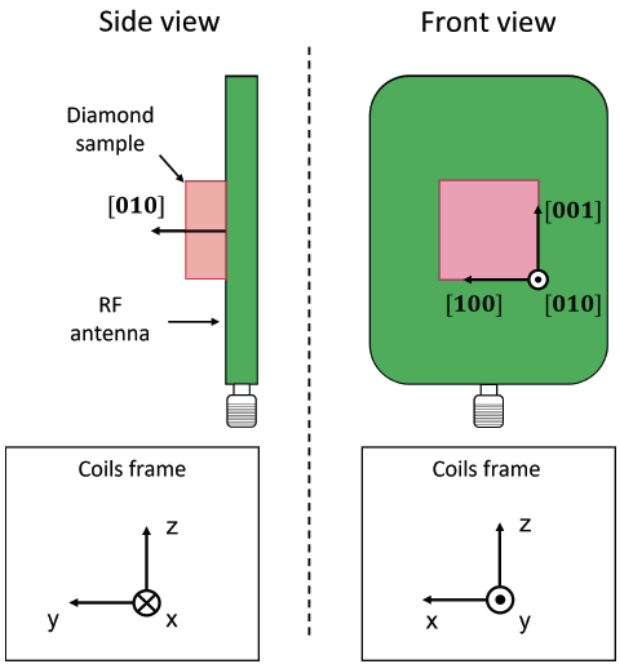

Figure 4.5 – Diagram of the sample orientation within the coils applying the magnetic field. The diamond is cut perpendicular to the orientation [010] - each of the 3 axes of the coils corresponds to one of the crystalline axes of the diamond lattice.

The diamond sample is oriented along the axes shown in figure 4.5. The aim of this section is to study the effect of field orientation on the ODMR spectra.

Q4. Recall the possible orientations of the NV centers in the crystal axis system. Associate with each of these orientations a unit vector in the X, Y and Z axis system of the coils.

Apply a field of around 2 mT along the Y axis, the sample normal.

Q5. What is the projection of this field onto the 4 possible orientations of the NV center? Use your answer to comment on the shape of the ODMR spectrum obtained.

Q6. If the magnetic field had a different projection on each of the 4 possible NV center orientations, what would we observe? Try to identify a field orientation compatible with the observation of a maximum number of peaks.

Q7. Choose one of the possible NV center orientations and suggest the current values to be applied to the coils to generate a magnetic field aligned with this orientation. Once the field has been applied, justify the number of peaks observed in the ODMR spectrum.

5.4 Mesasuring the gyromagnetic ratio

The aim of this section is to study the influence of the field norm on Zeeman splitting, for a class of NV centers with a given orientation.

- Pilotez les bobines pour observer le splitting sur la classe de défauts orientés selon [111]. L'alignement du montage et de l'échantillon ne sont pas nécessairement optimaux : pour aligner du mieux possible le champ B sur la bonne orientation, il est possible de procéder par tâtonnements en changeant légèrement les courants des bobines une fois une première orientation satisfaisante trouvée.

- Une fois la direction du champ fixée, scannez la norme du champ dz 0.6 à 2.8 mT (par exemple, 6 points). Vous devriez obtenir un spectre contenant 4 pics principaux.

Q8. To which origin do you attribute the 4 peaks in question?

Q9. Measure, for each applied field standard, the frequency of the most distant peaks) and plot them on a graph as a function of field standard. Use your measurements to calculate a value for the gyromagnetic ratio and a value for zero-field frequency splitting.

5.5 Measuring the Earth magnetic field

In reality, the magnetometer never rests in exactly zero field, even when the coils are switched off: it's bathed in the Earth's magnetic field. But this field is weak, and the Zeeman effect it generates is negligible compared with the spectral widths measured by ODMR.

The aim of this section is to determine the norm and orientation of this magnetic field. More generally, the method you are about to follow can be used to measure and characterize weak, unknown magnetic fields on very small scales.

Measurement guidelines

Measuring a magnetic field with a magnetometer is based, on the one hand, on the idea that the Zeeman splitting of a pair of peaks is linked to the norm of the projection of the magnetic field on the direction associated with an NV center, and on the other hand, on the exploitation of the 4 possible NV center orientations to obtain 4 different projections of the same magnetic field vector on different directions.

In the case of the Earth's magnetic field, its amplitude is too small to create an easily measurable Zeeman splitting. In addition, it should be noted that the 4 different splits are only separately measurable and identifiable if the field norm is sufficient (in which case the 4 pairs of peaks appear effectively separated and distant from each other on the ODMR spectrum).

The magnetic field of the coils is therefore added to that of the earth's magnetic field to obtain adequate ODMR spectra.

- A first spectrum is acquired with coils switched on so that the NV centers see a total magnetic field $\vec{B}^{+}_{tot} = \vec{B}_{Earth} + \vec{B}_{coils}$, revealing 4 pairs of peaks;

-

- A second spectrum is acquired by reversing the direction of the applied magnetic field, so that the total field becomes $\vec{B}^{-}_{tot} = \vec{B}_{Earth} - \vec{B}_{coils}$.

- We reconstruct the orientation of each of the measured fields $\vec{B}^{+}_{tot}$ and $\vec{B}^{-}_{tot}$ using the projections onto each of the 4 NV orientations.
-
- By sum,$\vec{B}_{Earth} = \frac{1}{2}\left(\vec{B}^{+}_{tot} + \vec{B}^{-}_{tot}\right)$

The field reconstruction procedure is detailed in the appendix to this document.

Experimental protocole

- Apply a magnetic field that resolves each of the 4 peak pairs in the ODMR spectrum, i.e. with a different projection on each of the 4 NV center orientations. As an example, choose the orientation :

$$\vec{B}_{\text{coils}} = \begin{pmatrix} 1.112 \\ 0.522 \\ 2.000 \end{pmatrix} \text{mT}$$

- Acquire the ODMR spectrum, and use the spectrum processing interface to identify the frequencies of the 4 pairs of peaks, each corresponding to a crystal orientation. Calculate the splitting of each of these pairs.

- Reverse the direction of the magnetic field, and similarly acquire a second ODMR spectrum, identifying peak frequencies and splittings.

Q11. Use the National Centre for Environmental Information website to find the value and local orientation of the Earth's magnetic field for TP: https://www.ngdc.noaa.gov/geomag/calculators/magcalc.shtml

Q10. Use the spectra processing interface to calculate the orientation of the magnetic field and compare your results. What uncertainties should you take into account when weighting your measurement? Comment on the main sources of uncertainty in your setup, and suggest ways of reducing them.

6 Appendix: magnetic field reconstruction

6.1 Expression of Zeeman splitting as a function of magnetic field projections

To reconstruct the magnetic field from ODMR spectra, each ODMR line must first be assigned an NV center class and orientation. To do this, we need to go back to the projection of the magnetic field onto each orientation.

The two split frequencies $f_{i_\pm}$ associated with a given NV center orientation $\mathbf{n_i}$ are expressed as :

$$f_{i_\pm} = f_0 \pm \gamma |\mathbf{B}_{\text{tot}}| \cos\theta_i \tag{4.5}$$

with $theta_i$ the angle between the magnetic field vector and the crystal orientation vector.

In the approximation where the terrestrial chap is much weaker than that applied by the coil, this angle is given by :

$$\frac{\mathbf{B_{coil}} \cdot \mathbf{n_i}}{|\mathbf{B_{coil}}||\mathbf{n_i}|} \approx \cos\theta_i \tag{4.6}$$

The sign matters and the cosine can be negative, so that $f_{i_+} > f_{i_-}$ if $\cos\theta_i > 0$, and $f_{i_+} < f_{i-}$ if $\cos\theta_i < 0$. Zeeman splitting, which can be positive or negative, is then expressed as :

$$\Delta f_i = |f_{i_+} - f_{i_-}| \times \text{sign}(\cos\theta_\text{i}) \tag{4.7}$$

6.2 Measuring a magnetic field component

In the labwork, two consecutive spectra are measured by reversing the direction of the magnetic field, resulting in two splitting measurements.

$$\mathbf{B}_{\text{tot}} = \mathbf{B}_{\text{Earth}} + \mathbf{B}_{\text{coil}} \longrightarrow \Delta f_i^+$$

$$\mathbf{B}_{\text{tot}} = \mathbf{B}_{\text{Earth}} - \mathbf{B}_{\text{coil}} \longrightarrow \Delta f_i^-$$

Using the projection angle θ_i, we can write :

$$\Delta f_i^+ = 2\gamma B_{\text{Earth}} \times \cos\theta_i + 2\gamma B_{\text{coil}} \times \cos\theta_i \tag{4.8}$$

1nd likewise,

$$\Delta f_i^- = 2\gamma B_{\text{Earth}} \times \cos\theta_i - 2\gamma B_{\text{coil}} \times \cos\theta_i \tag{4.9}$$

Combining the two expressions gives :

$$\frac{\Delta f_i^+ + \Delta f_i^-}{4} = B_{\text{Earth}} \times \cos\theta_i = B_{\text{Earth,i}} \tag{4.10}$$

i.e. the measurement of the projection of the value of the earth's magnetic field on the direction $\mathbf{n_i}$.

6.3 Crystal orientations and field reconstruction

The orientations of the various NV center classes can be linked to the axes of the laboratory's frame of reference $\mathbf{n}_\alpha$,$\mathbf{n}_\beta$, $\mathbf{n}_\delta$,$\mathbf{n}_\gamma$

$$[111] \longrightarrow \mathbf{n}_\alpha = \frac{1}{\sqrt{3}} \begin{pmatrix} 1 \\ 1 \\ 1 \end{pmatrix}$$

$$[\bar{1}\bar{1}1] \longrightarrow \mathbf{n}_\beta = \frac{1}{\sqrt{3}}\begin{pmatrix}-1\\-1\\1\end{pmatrix}$$
$$[\bar{1}11] \longrightarrow \mathbf{n}_\delta = \frac{1}{\sqrt{3}}\begin{pmatrix}-1\\1\\1\end{pmatrix}$$
$$[1\bar{1}1] \longrightarrow \mathbf{n}_\gamma = \frac{1}{\sqrt{3}}\begin{pmatrix}1\\-1\\-1\end{pmatrix}$$

This translates directly into a system of equations linking the Cartesian components of the field to those projected onto the crystal orientations:

$$\begin{aligned}
\sqrt{3} \times B_{\mathrm{Earth},\alpha} &= +B_{\mathrm{Earth,x}} + B_{\mathrm{Earth,y}} + B_{\mathrm{Earth,z}} \\
\sqrt{3} \times B_{\mathrm{Earth},\beta} &= -B_{\mathrm{Earth,x}} - B_{\mathrm{Earth,y}} + B_{\mathrm{Earth,z}} \\
\sqrt{3} \times B_{\mathrm{Earth},\delta} &= -B_{\mathrm{Earth,x}} + B_{\mathrm{Earth,y}} + B_{\mathrm{Earth,z}} \\
\sqrt{3} \times B_{\mathrm{Earth},\delta} &= +B_{\mathrm{Earth,x}} - B_{\mathrm{Earth,y}} - B_{\mathrm{Earth,z}}
\end{aligned}$$

which gives :

$$\begin{aligned}
B_{\mathrm{Earth,x}} &= \frac{\sqrt{3}}{4}(B_{\mathrm{Earth},\alpha} - B_{\mathrm{Earth},\beta} - B_{\mathrm{Earth},\delta} + B_{\mathrm{Earth},\gamma}) \\
B_{\mathrm{Earth,y}} &= \frac{\sqrt{3}}{4}(B_{\mathrm{Earth},\alpha} - B_{\mathrm{Earth},\beta} + B_{\mathrm{Earth},\delta} - B_{\mathrm{Earth},\gamma}) \\
B_{\mathrm{Earth,z}} &= \frac{\sqrt{3}}{4}(B_{\mathrm{Earth},\alpha} + B_{\mathrm{Earth},\beta} + B_{\mathrm{Earth},\delta} + B_{\mathrm{Earth},\gamma})
\end{aligned}$$

P 5

Spectroscopy of a jet of atoms

This lab illustrates the first stage of laser atom cooling experiments, namely the production of a jet of atoms from an oven, which will then be captured in a magneto-optical trap. You will carry out spectroscopy of the jet of atoms using a laser, most specifically the absorption and fluorescence spectroscopy of a line of the hyperfine structure of rubidium 85 around $780\,\mathrm{nm}$.

Contents

P1 Fluorescence rate of a two-level atom.

In this tutorial, atoms will be modelled as two-level systems. The interaction between a laser beam and a two-level atom is described by the optical Bloch equations (OBE). The stationary solution of the OBEs for the fraction of atoms in the excited state is given by

$$\Pi_e = \frac{1}{2}\frac{s}{1+s}\,, \tag{5.1}$$

where the saturation parameter writes

$$s = \frac{I/I_s}{1+4\Delta^2/\Gamma^2}\,, \tag{5.2}$$

as a function of the laser detuning to the atomic transition

$$\Delta = (\omega - \omega_0) - \mathbf{k}\cdot\mathbf{v}\,. \tag{5.3}$$

The fraction of atoms in the ground state is simply deduced from that in the excited state:

$$\Pi_g = 1 - \Pi_e. \tag{5.4}$$

In the equations above, we have used the following notations:

- ω, I and $\mathbf{k}$ are respectively the pulsation of the laser beam, its intensity and its wave vector;
- ω_0, I_s and $1/\Gamma$ are respectively the Bohr pulsation of the atomic transition, its saturation intensity and the lifetime of the excited state.
- $\mathbf{v}$ is the velocity of the atom in the laboratory reference frame.

Finally, remember that the fluorescence rate of a two-level atom is equal to $\Pi_e\Gamma$.

Q1 Name the function representing the fluorescence spectrum of an atom, i.e. the change in fluorescence rate as a function of detuning. Determine its total width at half-maximum in the low-intensity limit. $I \ll I_s$.

Q2 Explain why the fluorescence and absorption spectra of the laser by an atom have an identical profile as a function of the laser detuning.

Q3 What effect causes the term $-\mathbf{k}\cdot\mathbf{v}$ in the expression of the detuning Δ (Equation 5.3) ?

Q4 In a gas at equilibrium at a temperature T, the fluorescence spectrum broadened by the Doppler effect has a total width at half-maximum equal to

$$\Delta\omega = \sqrt{8\ln 2}\,\sqrt{\frac{k_B T}{m}}\,\frac{\omega_0}{c}. \tag{5.5}$$

In this equation, $k_B = 1.38\times10^{-23}$J/K is Boltzmann's constant, $m = 1.41\times10^{-25}$ kg is the mass of a rubidium atom and c is the speed of light in vacuum.
Calculate the Doppler shift expected in a cell at room temperature ($T \sim 20°$C) for the rubidium line centred at $780\,\mathrm{nm}$.

P2 Distribution of velocities in the jet of atoms.
The jet of atoms is obtained from a rubidium vapour produced by heating a metal sample in an oven to a temperature of $T \simeq 100\,°\mathrm{C}$. This vapour escapes from the oven through a first circular orifice of diameter $D_1 = 5\,\mathrm{mm}$. A second orifice of diameter $D_2 = 1\,\mathrm{cm}$ placed at a distance $L \simeq 20\,\mathrm{cm}$ from the first one filters the distribution of transverse velocities, thus creating an atomic jet.

Q5 Assuming that the gas is at thermodynamic equilibrium in the oven, give the energy distribution of the atoms, then their velocity distribution, expressed as a function of the norm of the velocity vector $v = \|\mathbf{v}\|$.

Q6 Estimate numerically the average $\langle v\rangle = \sqrt{9\pi k_B T/8m}$ of the norm of the velocity vector at the exit of the oven.

Q7 Assuming that the velocity of an atom along the axis of the circular orifices is equal to $\langle v \rangle$, estimate the maximum transverse velocity that will allow this atom to reach the last chamber. To make the calculation easier, consider that $D1 = D2 = 1\,\mathrm{cm}$.

1 Absorption spectrum

In this section you will first measure the absorption spectrum of a laser beam of wavelength $780\,\mathrm{nm}$ through a spectroscopy cell at room temperature, then through the jet of atoms produced by the oven. The optical set-up is shown in figure 5.1 below.

The natural abundance of the two isotopes of Rubidium is $\sim 72.2\%$ for the 85 isotope and $\sim 27.8\%$ for the 87 isotope..

IMPORTANT Make sure the laser diode is set to the following values: selected current (« set ») $I_{\text{set}} = 143{,}5\,\mathrm{mA}$ and set temperature $T_{\text{set}} = 19{,}550\,^{\circ}\mathrm{C}$.

Absorption spectrum through the cell at room temperature

$\rightsquigarrow$ Scan the laser diode current using the RIGOL function generator connected to the external modulation input of the laser diode controller and display on the oscilloscope 4 resonances such as those shown in figure 5.2. To do this, choose a symmetrical triangular sweep pattern, a modulation frequency of the order of $100\,\mathrm{Hz}$ and a peak-to-peak modulation amplitude of the order of $300\,\mathrm{mV}$ (and a zero offset voltage).

Each of these resonances actually comprises several unresolved atomic transitions: the difference in energy between the hyperfine sub-states of the excited state is smaller than the Doppler shift at ambient temperature.
An energy diagram of the hyperfine structure of rubidium isotopes 85 and 87 is given in the appendix.

Q8 The lines observed in Figure 3 are identified through the isotope (85 or 87) and the F hyperfine state of the ground state. Justify this identification by checking that the relative distance between the two lines of each isotope corresponds to what is expected from the energy diagrams.

Q9 Using the same data, determine the coefficient of proportionality between the current modulation voltage and the optical frequency of the laser.

Q10 Measure the total width at half-maximum of the two rubidium 85 resonances. Compare your result with the natural width expected for a transition, i.e. $\Gamma/2\pi = 6{,}1\,\mathrm{MHz}$, and with the width calculated in question Q4.
Comment your result.

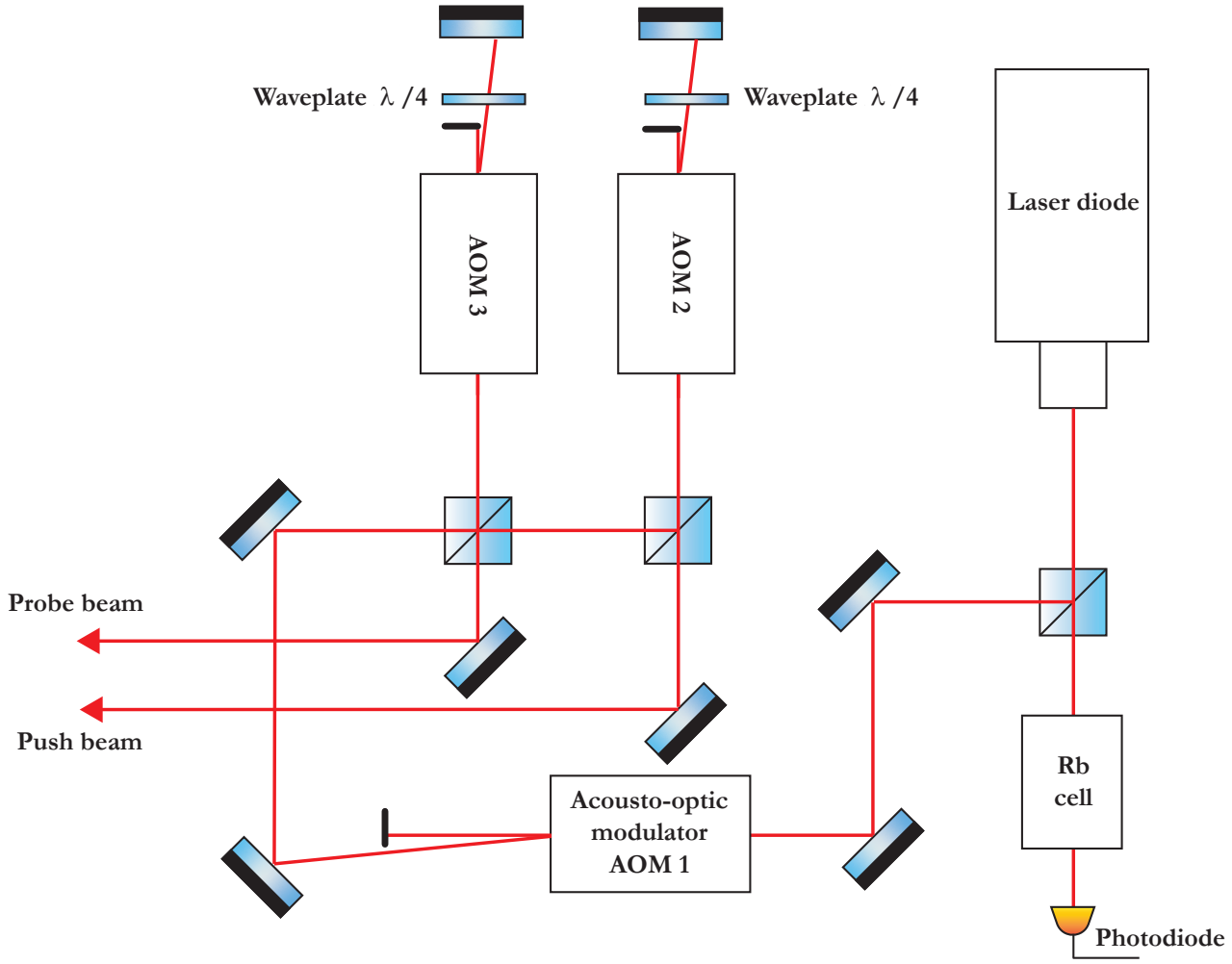

Figure 5.1 – Description of the optical table. The light source is a laser diode emitting around $780\,\mathrm{nm}$. Part of the beam is used for spectroscopy in the glass cell. The other part of the beam is sent through a first single-pass AOM. The laser beam is then split into two beams, each injecting a double-pass AOM. The probe and push beams thus generated are sent to the vacuum chamber.

Absorption spectrum through the jet of atoms In this section, you will measure the absorption spectrum of a jet of rubidium atoms using the probe beam shown in figure 5.3.

Initial settings. The AOM2 and AOM3 acousto-optic modulators are driven using the SIGLENT arbitrary function generator, which has two output channels. It will be ensured for both output channels that a sinusoid of frequency $200\,\mathrm{MHz}$ and amplitude $100\,\mathrm{mV}$ is sent to the two acousto-optic modulators.

$\rightsquigarrow$ Simultaneously observe the signals from the photodiodes in the cell and the jet using an oscilloscope.

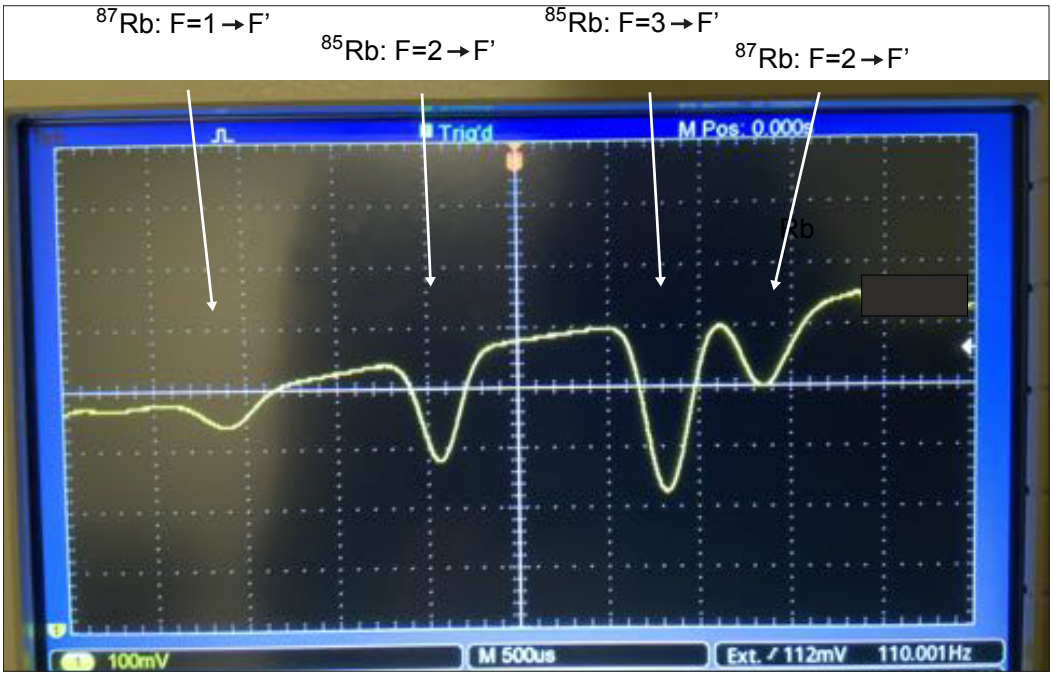

Figure 5.2 – Absorption spectrum in the cell. This spectrum was obtained using the same set-up as the one you have, by measuring the laser intensity transmitted through the cell using an amplified photodiode and sweeping the frequency of the laser diode. It shows 4 lines linked to the hyperfine structure of the 85 and 87 isotopes of rubidium around $780\,\mathrm{nm}$ (see the energy diagrams in the appendix).

Q11 What obvious difference(s) can you see between the two absorption signals?

⇝ Modify the amplitude of the laser diode current sweep so that only the most intense absorption line is observed in the cell. The absorption spectrum from the jet of atoms should now look like that shown in figure. 5.4.

Q12 Using the energy diagrams given in the appendix, identify the atomic transitions visible in the absorption spectrum of the jet of atoms.

Q13 Measure the total width at half-maximum of the most intense absorption line across the jet.
From the expression for Doppler broadening given in equation 5.5, estimate an "effective" temperature corresponding to your linewidth measurement. Why can't this be a 'true' temperature?

Q14 Discuss the value of the atom jet for spectroscopic measurements.

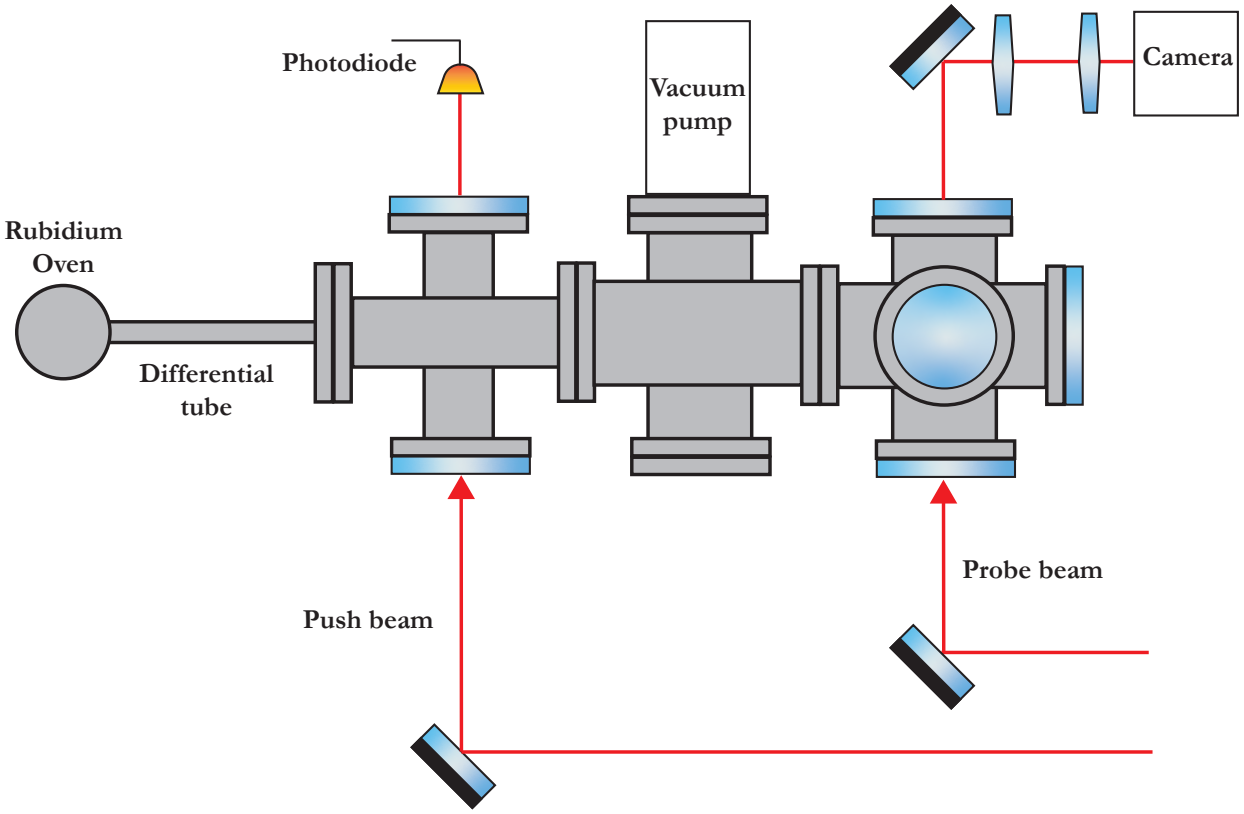

Figure 5.3 – Description of the vacuum chamber. The jet of rubidium atoms is produced in an oven heated to around 100 °C and whose outlet is bounded by a narrow cylinder. The jet propagates from left to right in the diagram. The transverse velocity distribution of the jet is characterised in the rightmost chamber, either by absorption of the probe beam using a photodiode (not shown), or by fluorescence induced by the same probe beam using a camera. In the intermediate chamber, a push beam can deflect the atomic beam before it reaches the probe.

Q15 Give a rough estimate of the frequency resolution achieved by external modulation of the laser diode current.
In the next section, we will see that this resolution limit can be greatly reduced by using an acousto-optic modulator (AOM) to sweep the laser beam frequency.

2 Fluorescence spectrum

You are now going to observe the fluorescence spectrum of the atomic jet using a camera positioned perpendicular to the probe beam.

⇝ Using modulation of the laser diode current to vary the frequency of the laser beam (procedure identical to the previous section), observe the fluorescence resonance on the camera.

Figure 5.4 – Absorption spectrum through the atomic jet. This spectrum was obtained using the same set-up as the one you have, by measuring the laser intensity transmitted through the vacuum chamber and the atomic jet, using an amplified photodiode and sweeping the frequency of the laser diode.

Q16 Determine the orientation of the probe beam and the jet of atoms on the camera image.

⇝ Disable the laser diode current sweep and add a $50\,\Omega$ termination to the controller's external modulation input. Slowly modify (a few MHz at a time) the frequency of AOM No. 3 driven by the SIGLENT generator until the fluorescence resonance on the camera is restored.

⇝ Determine the frequency range that needs to be covered to visualise the entire fluorescence resonance, i.e. the minimum (respectively maximum) frequency below (respectively above) which the fluorescence signal is negligible.

Q17 What is the first observation you can make about the resolution of the frequency sweep performed using the AOM compared with that performed by modulating the laser diode current?

⇝ We want to measure the shape of the observed resonance precisely. To begin, acquire a fluorescence image using the camera control software. Elect an area of interest (ROI) covering the entire sensor in the direction of the laser beam but only the fluorescence signal in the

direction of the jet. Extract the average number of grey levels $N_{\text{n.g.}}$ calculated by the histogram function.

$\rightsquigarrow$ We also want to ensure that we are working within a linear response regime, defined by a saturation parameter s less than the unit.
To determine this regime in the experiment, we begin by choosing the AOM frequency for which the fluorescence signal (i.e. the average number of grey levels $N_{\text{n.g.}}$ in the ROI) is maximum. Keeping this frequency fixed, we vary the amplitude of the signal sent to the AOM by the SIGLENT generator: for each value of the amplitude chosen, we measure both $N_{\text{n.g.}}$ and the voltage V_{PD} on the photodiode of the probe beam.

Q18 Plot the curve $N_{\text{n.g.}}$ as a function of V_{PD} and identify the linear and saturated fluorescence regimes. Determine the maximum value of amplitude of the AOM drive signal below which the variation of $N_{\text{n.g.}}$ is linear with V_{PD}.

$\rightsquigarrow$ Measure the number of grey levels in the ROI as a function of the frequency of the AOM drive signal. Choose about ten frequency values spread over the range you determined in question Q16.

Q19 Plot the fluorescence spectrum obtained as a function of the AOM drive frequency. Determine its total width at half-height and compare it with that of the absorption spectrum by the jet of atoms. Be careful to take into account the double passage through the AOM, which shifts the laser beam frequency by twice the AOM drive frequency!

$\rightsquigarrow$ When the drive frequency of the AOM is varied, the diffraction efficiency changes as we move away from the Bragg condition. This effect is likely to alter the measurement of the fluorescence spectrum and can be corrected. To do this, measure V_{PD} as a function of AOM frequency over the range used for the previous measurement in order to calibrate the variation in optical power of the probe beam. Correct the fluorescence spectrum measurement to compensate for the effect of the variation in probe beam power.

Q20 Plot the corrected spectrum and compare it with the raw spectrum. Does it seem necessary to take into account the modulation of the optical power of the probe beam?

$\rightsquigarrow$ Reproduce the measurement of the fluorescence spectrum for the maximum value of the optical power of the probe beam and plot the new spectrum obtained.

Q21 Compare the width of this spectrum with that of the spectrum obtained at low power and comment on the effect of saturation.

3 OPTIONAL SECTION - Mechanical action of light on atoms

If you have time, you can deal with this optional section.

In this final section, we study the mechanical effect of laser light on the atomic jet. This effect is similar to that exerted by sunlight on the tail of a comet: the radiation pressure exerted by the sunlight bends the tail of the comet.

The radiation pressure force exerted by the laser light on the atom at two levels is written,

$$\mathbf{F}_{\text{rad}} = \hbar\mathbf{k}\frac{\Gamma}{2}\frac{s}{1+s} \ . \tag{5.6}$$

$\rightsquigarrow$ Add the pusher beam to the empty chamber at the end of the oven. Set the power of the push beam to its maximum and vary its frequency until an effect on the fluorescence resonance is observed.

Q22 Interpret the modification of the spectrum by the mechanical action of the laser beam at the oven outlet.

Q23 Estimate the variation in impulse experienced by an atom passing through a laser beam.

Q24 Discuss the best beam size for measuring the velocity distribution of the jet of atoms.

4 Annexe

Hyperfine structure of the D2 line of rubidium isotopes 85 and 87. The figures are taken from documents posted online by Daniel Steck at the following address http://steck.us/alkalidata/.

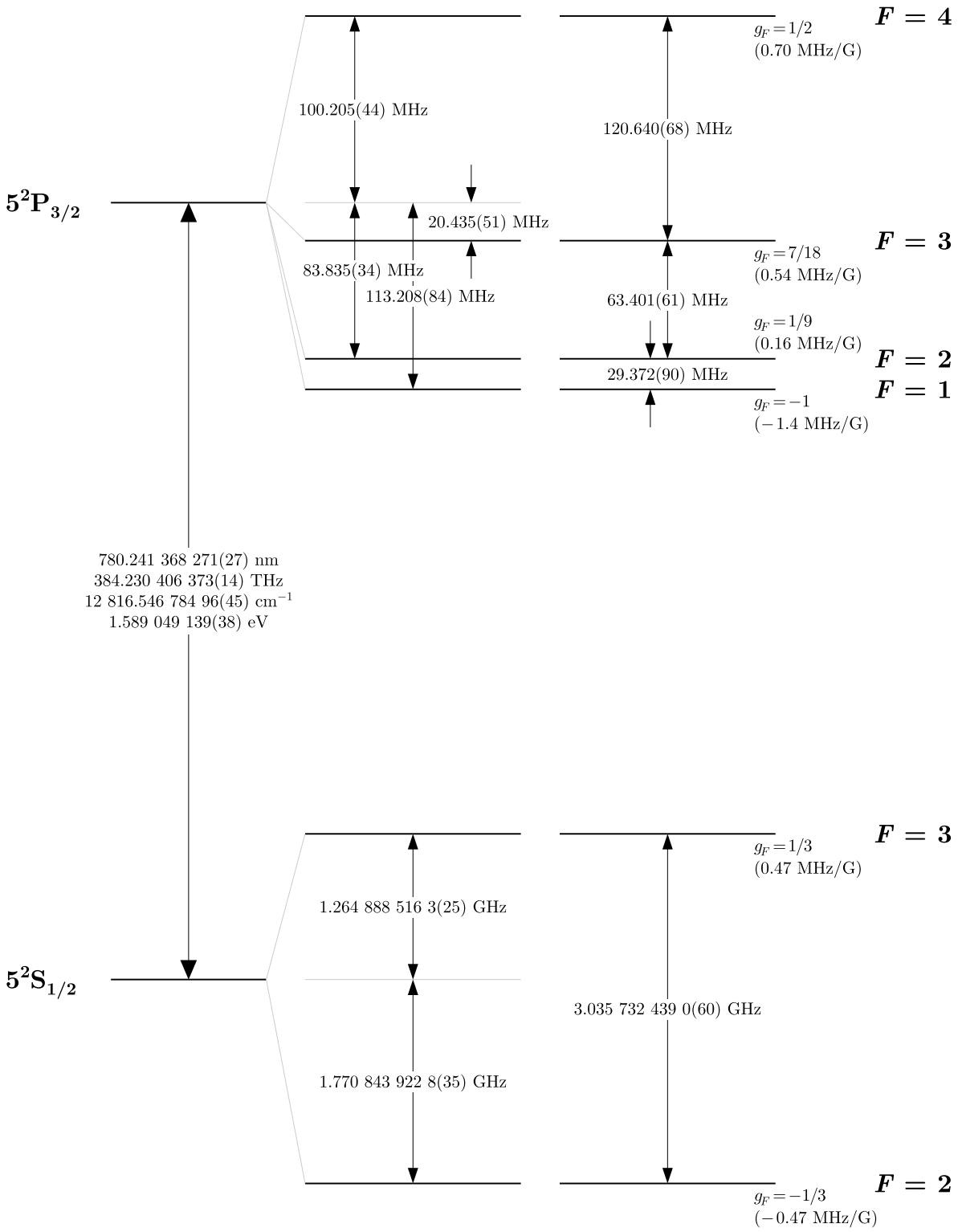

Figure 5.5 – Hyperfine structure of the D2 transition of rubidium 85.

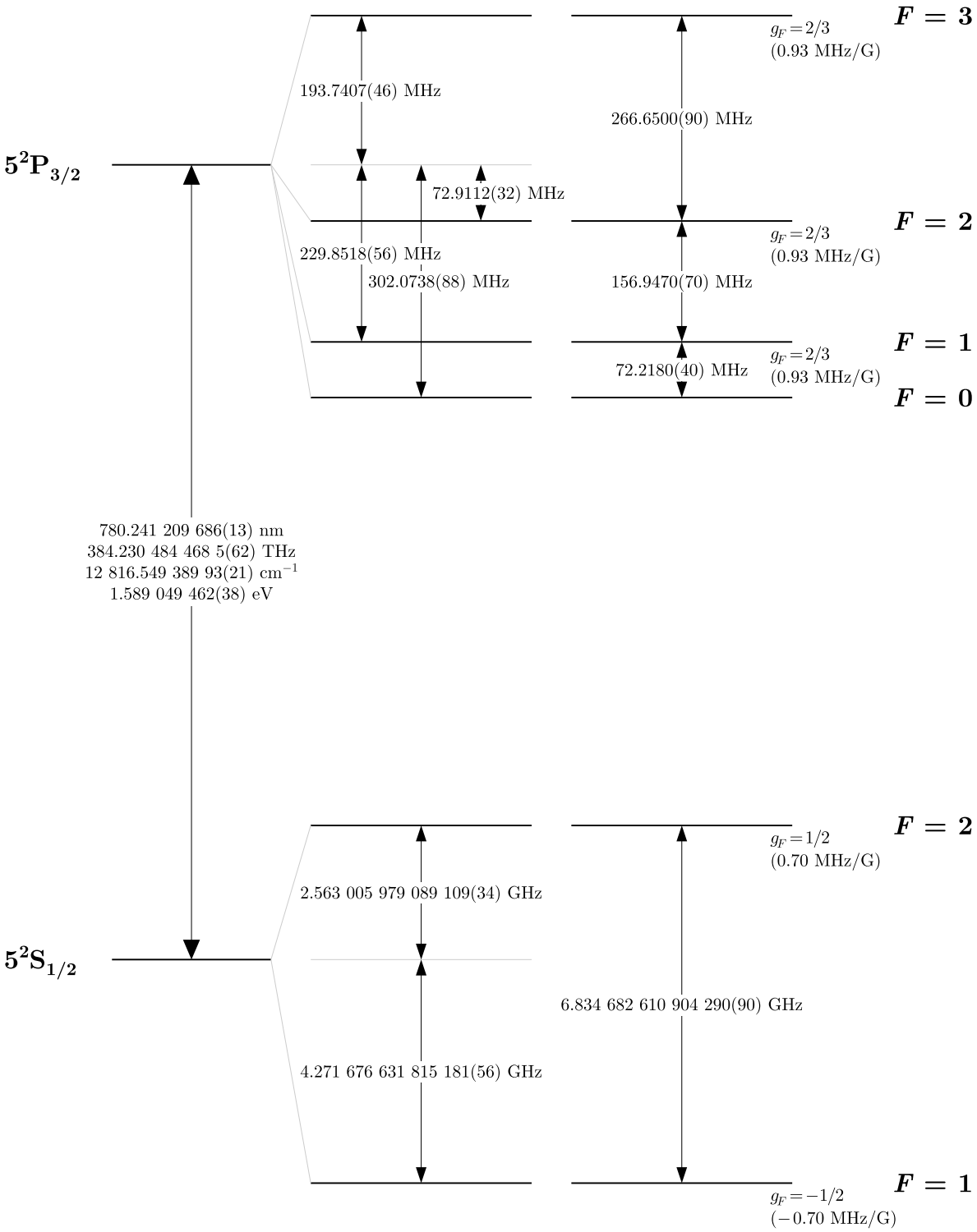

Figure 5.6 – Hyperfine structure of the D2 transition of rubidium 87.